Probing dense matter inside NSs through free precession and dynamical tides

Yong Gao

Max Planck Institute for Gravitational Physics, Potsdam

August 5–7, 2024

Outline

- Neutron stars (NSs): EoS and global properties of NSs
- Precession of NSs: modelling and observations
- Dynamical tides in BNS inspiral
- Summary and outlook

NS—Laboratory for extreme physics

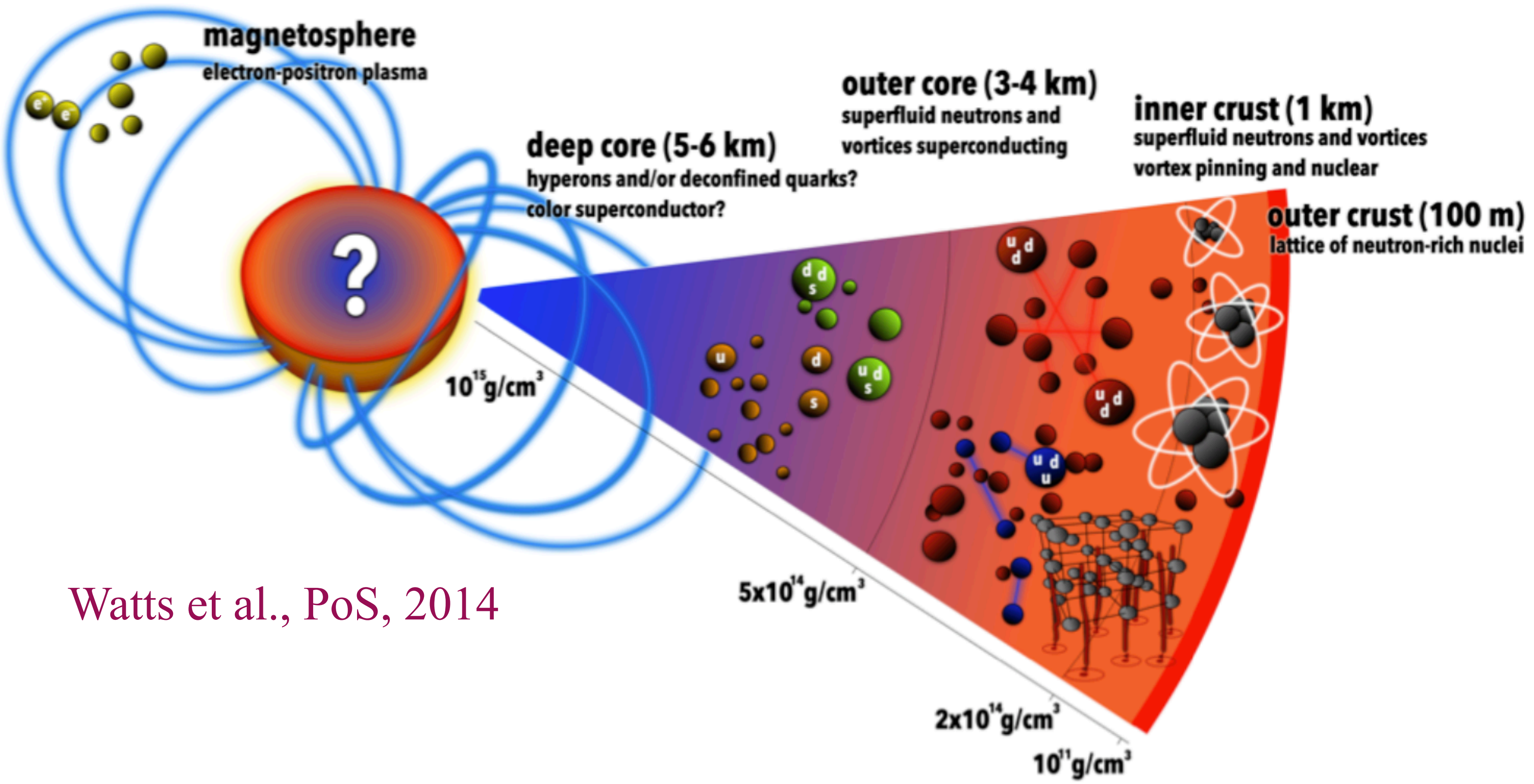

Watts et al., PoS, 2014

$$\frac{M}{R} \sim \frac{1.4\,M_\odot}{10\,\mathrm{km}} \sim 0.3$$

$$\bar{\rho} \sim (2-3)\rho_0$$

$$B \sim 10^{12}\,\mathrm{G}$$

$$T_\mathrm{F} \approx 10^{12}\left(\frac{\rho}{\rho_0}\right)^{2/3}\ \mathrm{K}$$

- **Gravity**, curves the spacetime, source for gravitational waves (GWs)
- **Strong interaction**, determines the internal composition and state
- **Electromagnetism**, makes pulsars' pulses and magnetars' flares
- **Weak interaction**, cools down the star

The many faces of NSs

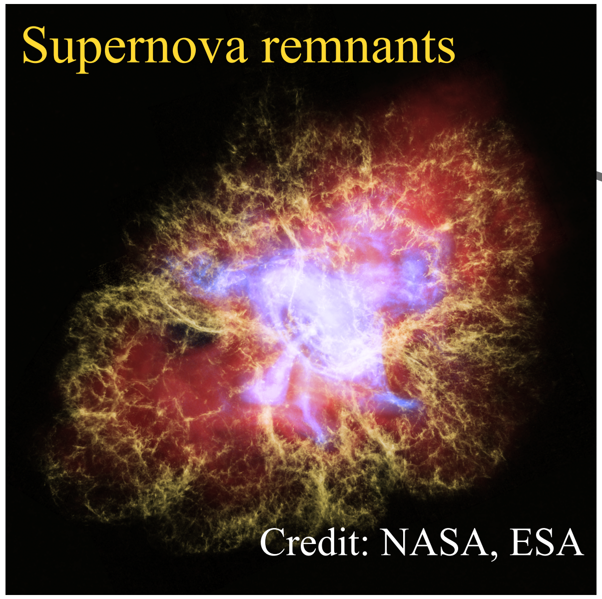

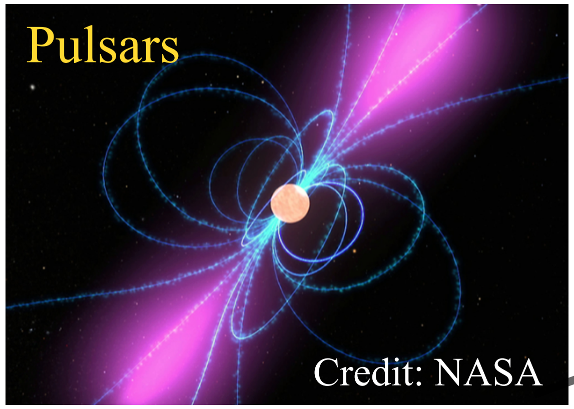

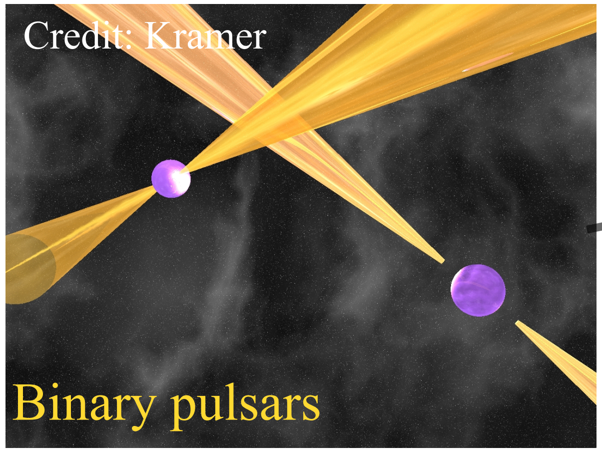

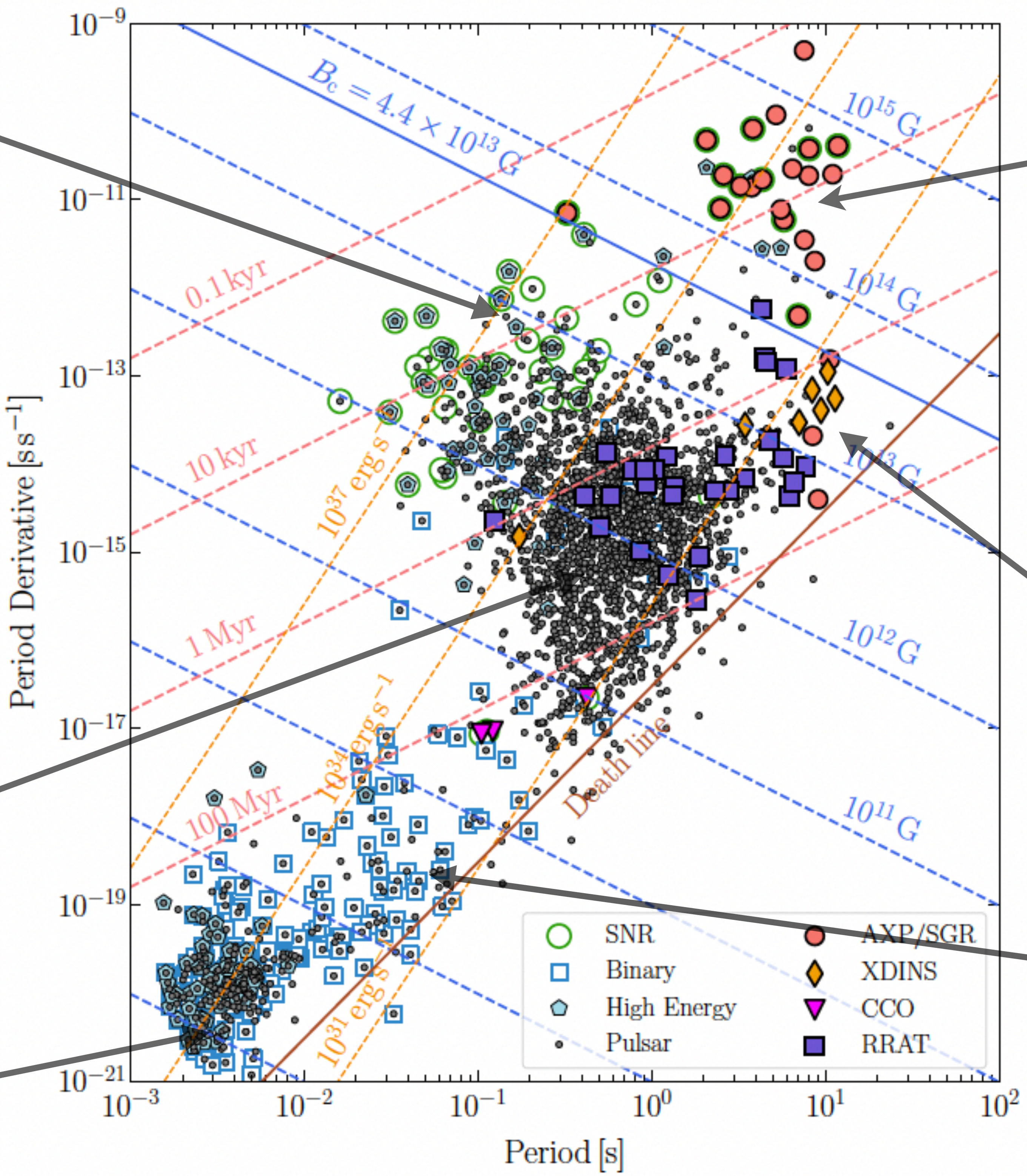

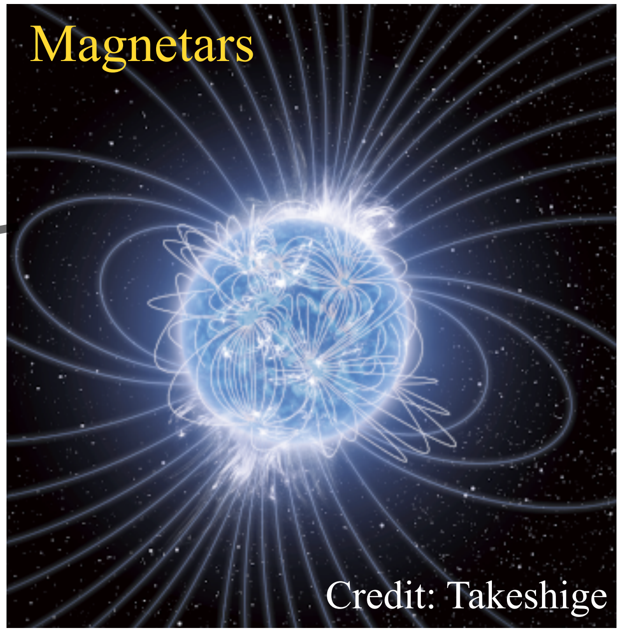

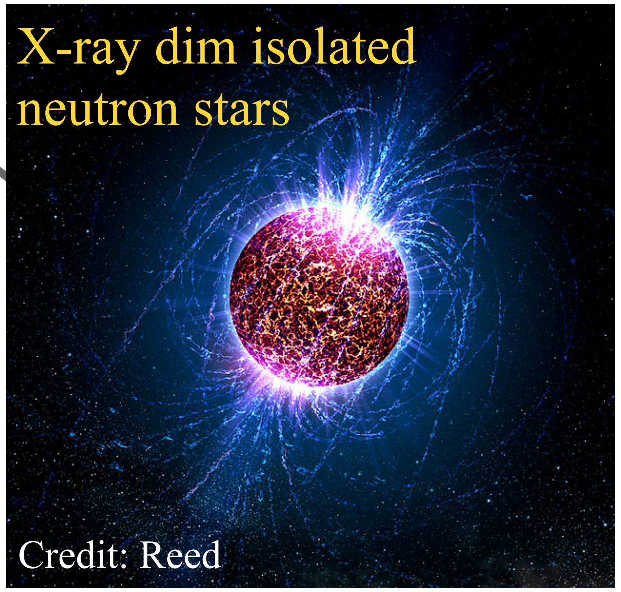

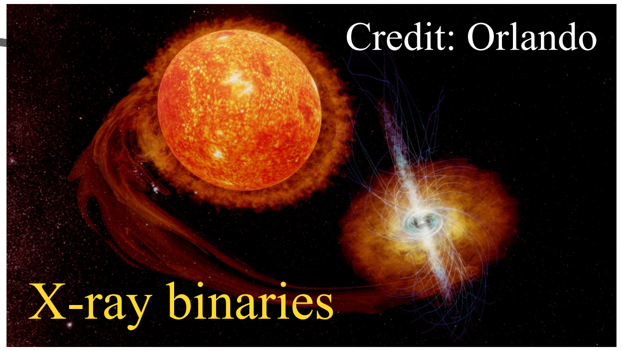

Data taken from ATNF Pulsar Catalog and McGill Catalog

GW170817 and multimessenger astronomy

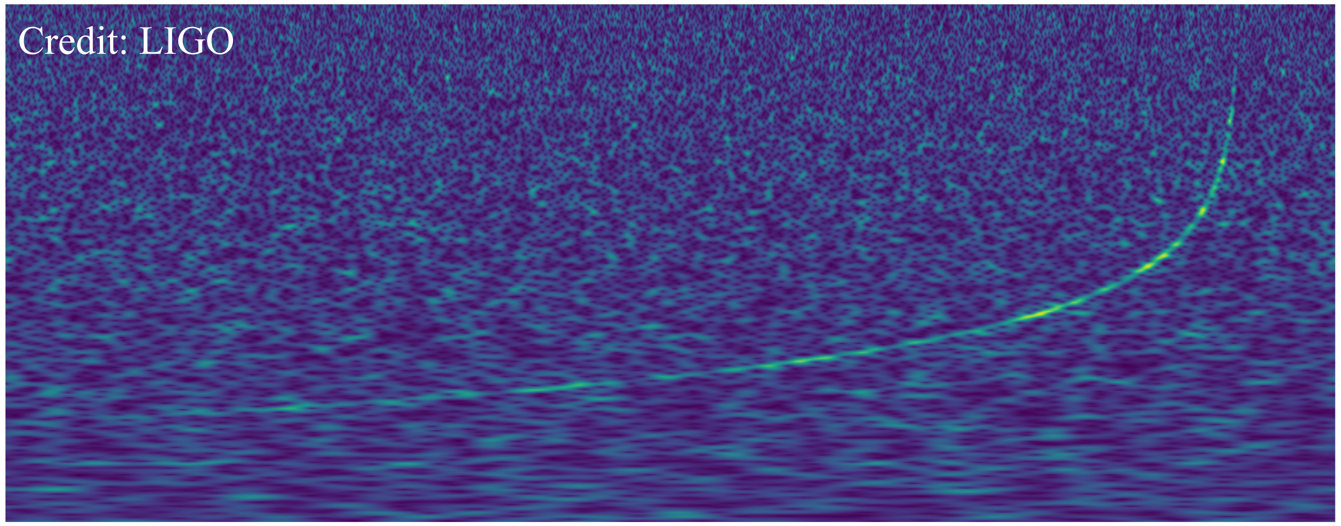

The "chirp sound" produced as the two NSs inspiral

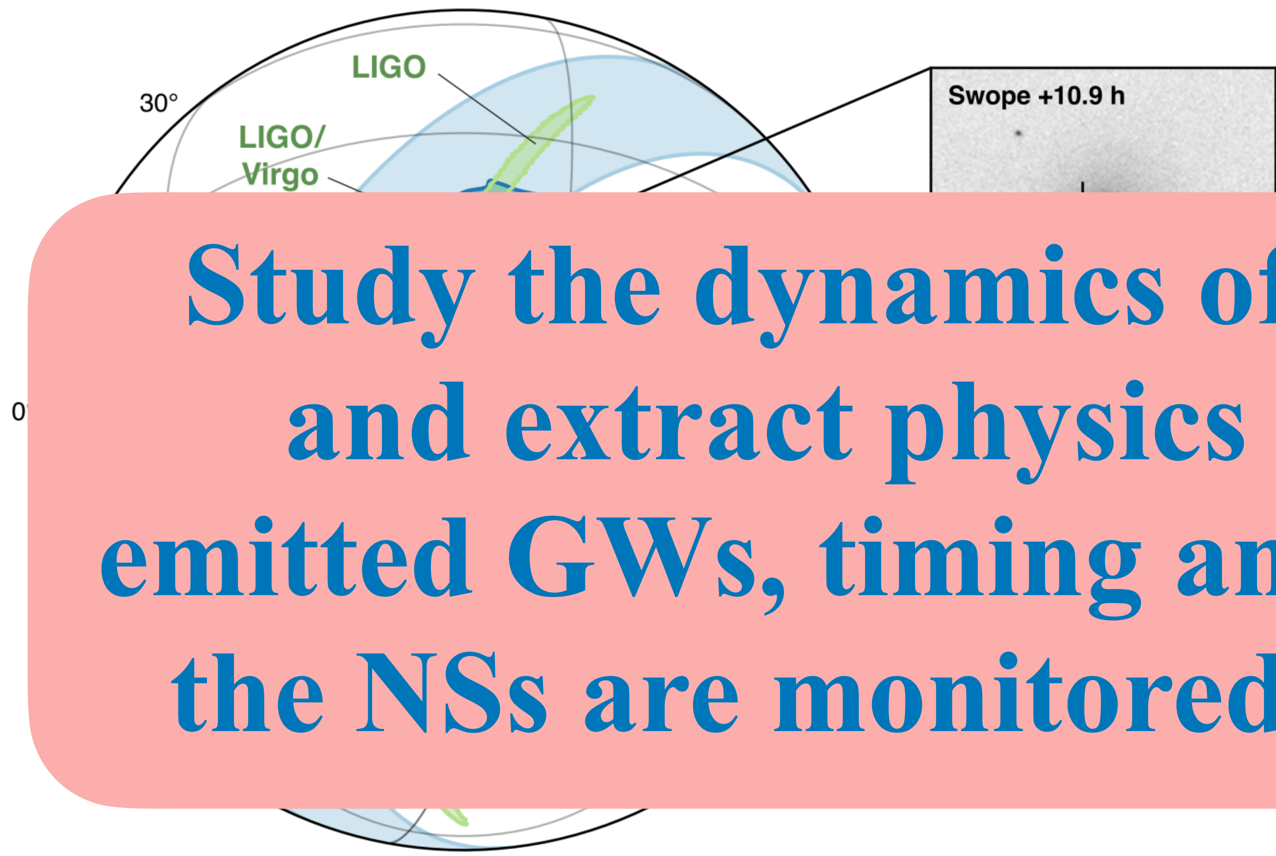

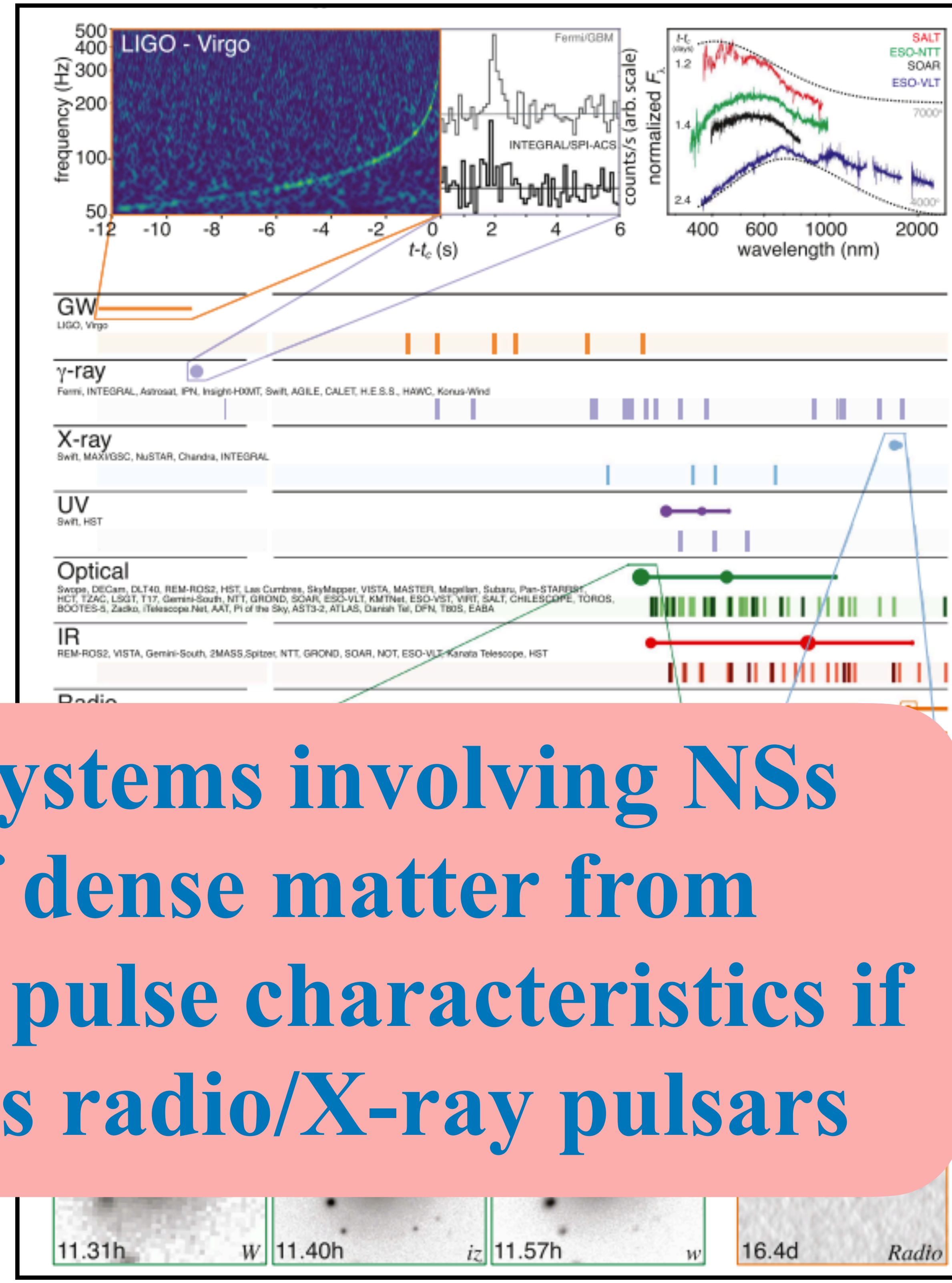

Study the dynamics of systems involving NSs and extract physics of dense matter from emitted GWs, timing and pulse characteristics if the NSs are monitored as radio/X-ray pulsars

Abbott et al., PRL, 2017

LIGO Scientific Collaboration et al., ApJL, 2017

The EoS models of NSs

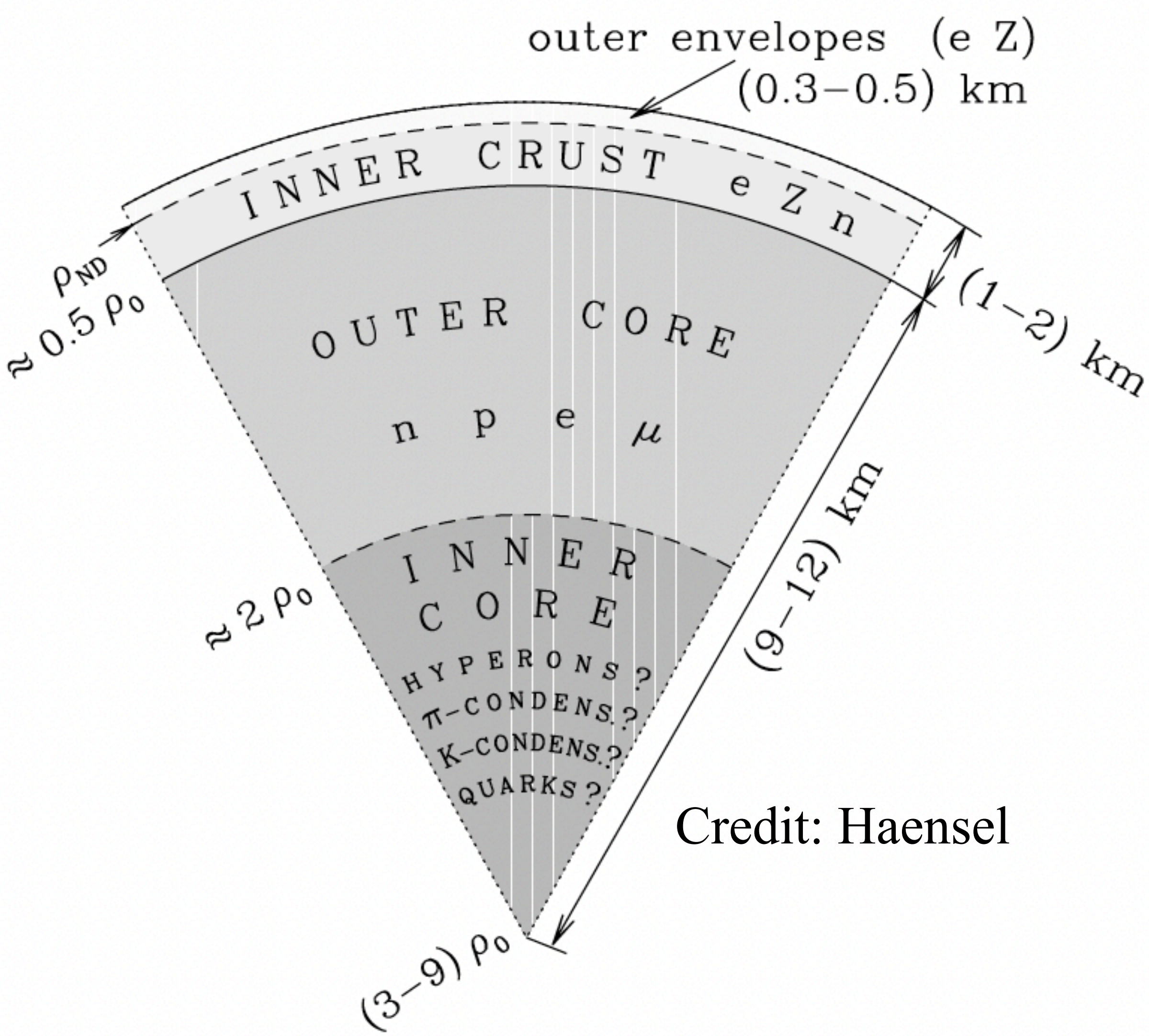

Credit: Haensel

Conventional NS models

- Nucleon star: *npeμ* matter
- New freedom in the inner core: hyperons? mesons? quarks?

- Strange quark matter (SQM)

Witten's conjecture: Quark matter composed of nearly equal number of *u*, *d*, *s* quarks is the ground state of strong matter

- Quark stars (QSs) in simple MIT bag model

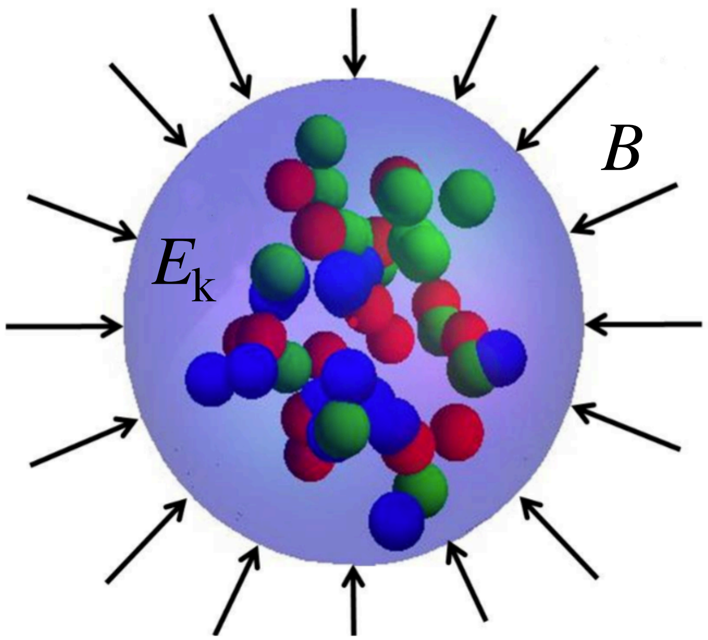

Credit: Köpp

Mass-radius relation of NSs

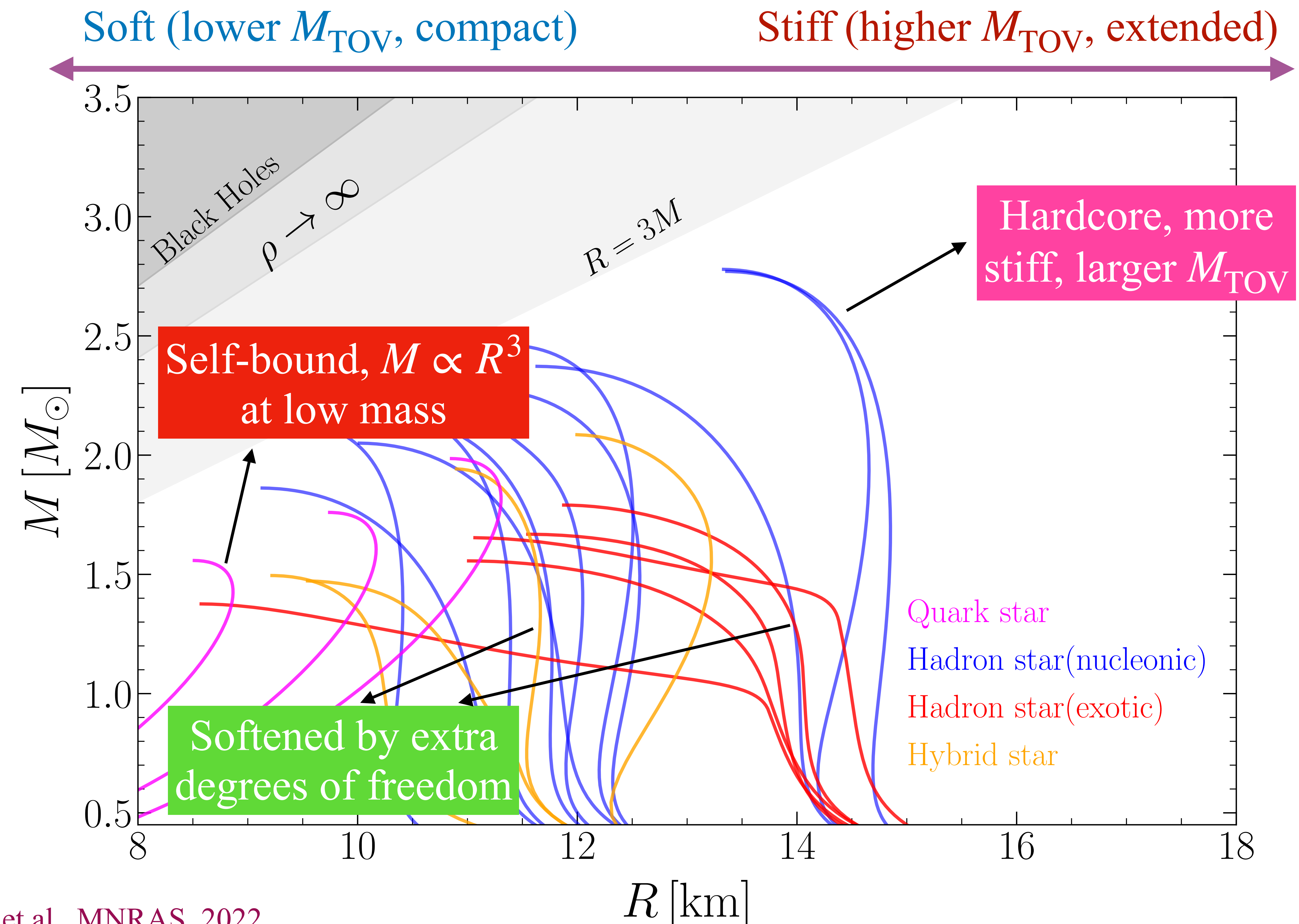

Gao et al., MNRAS, 2022

Mass-radius relation of NSs

- Non-pulsed emission from whole surface — measure surface area; Quiescent LMXBs, X-ray Bursts (Chandra, XMM, HXMT, Athena)

$$\frac{R_{\rm obs}}{D} = \left(\frac{F_{\rm bol}}{\sigma_{\rm B} T_{\rm eff}^4}\right)^{1/2} \qquad R_{\rm obs} = \left(1 - \frac{2GM}{Rc^2}\right)^{-1/2} R$$

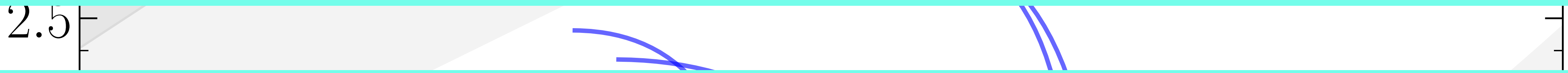

- Pulsed emission — look for effects of gravitational field (i.e. mass and radius) on time variations of flux; millisecond period X-ray pulsars (NICER)

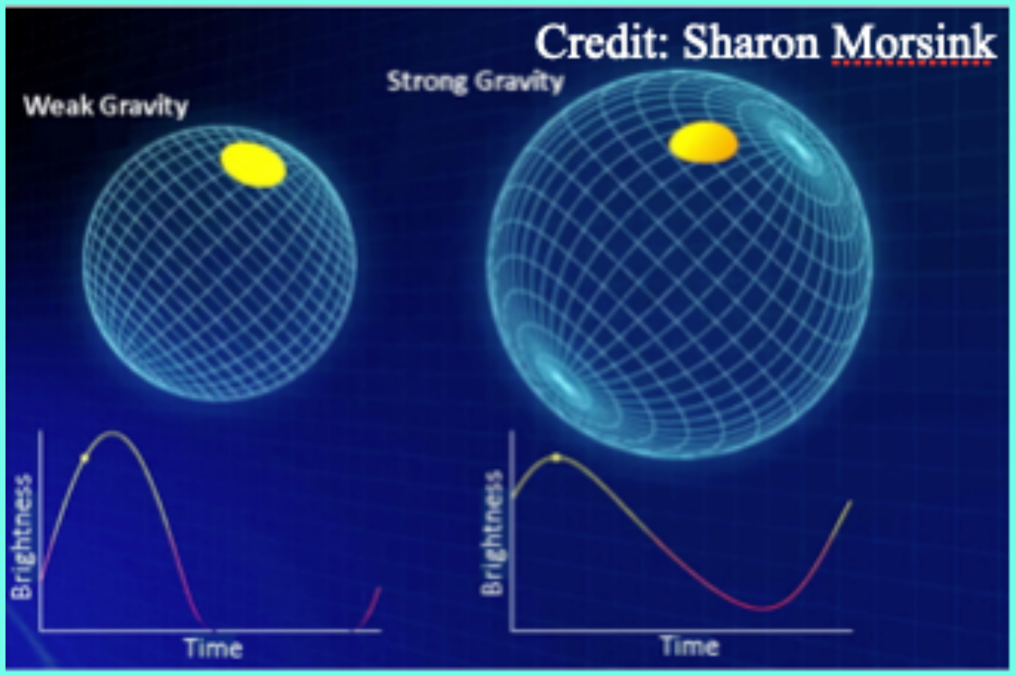

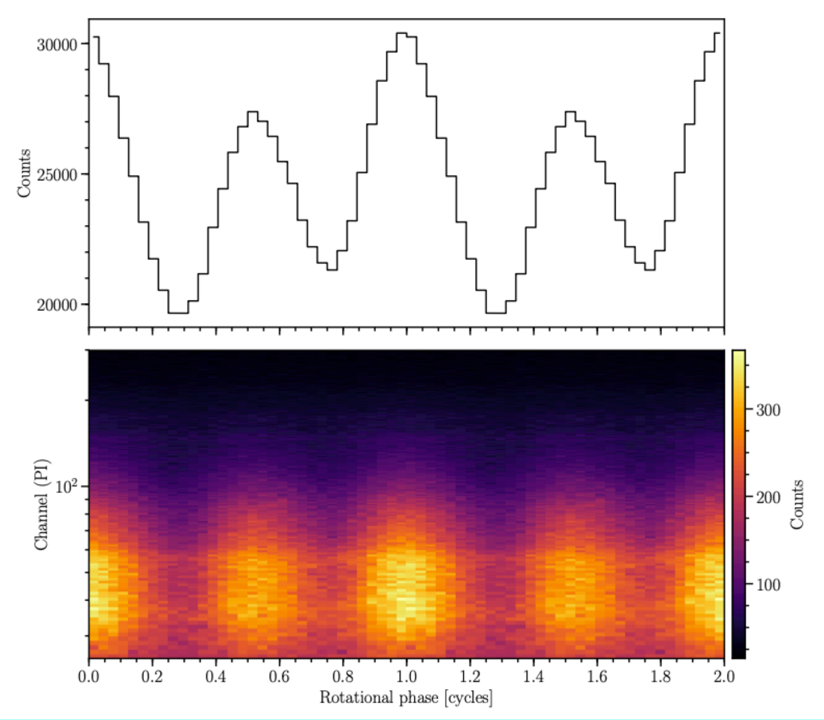

PSR J0030+0451

Riley et al., ApJL, 2019

$$R = 12.71^{+1.14}_{-1.19}\ \text{km}$$

Miller et al., ApJL, 2019

$$R = 13.02^{+1.24}_{-1.06}\ \text{km}$$

Deformed NSs

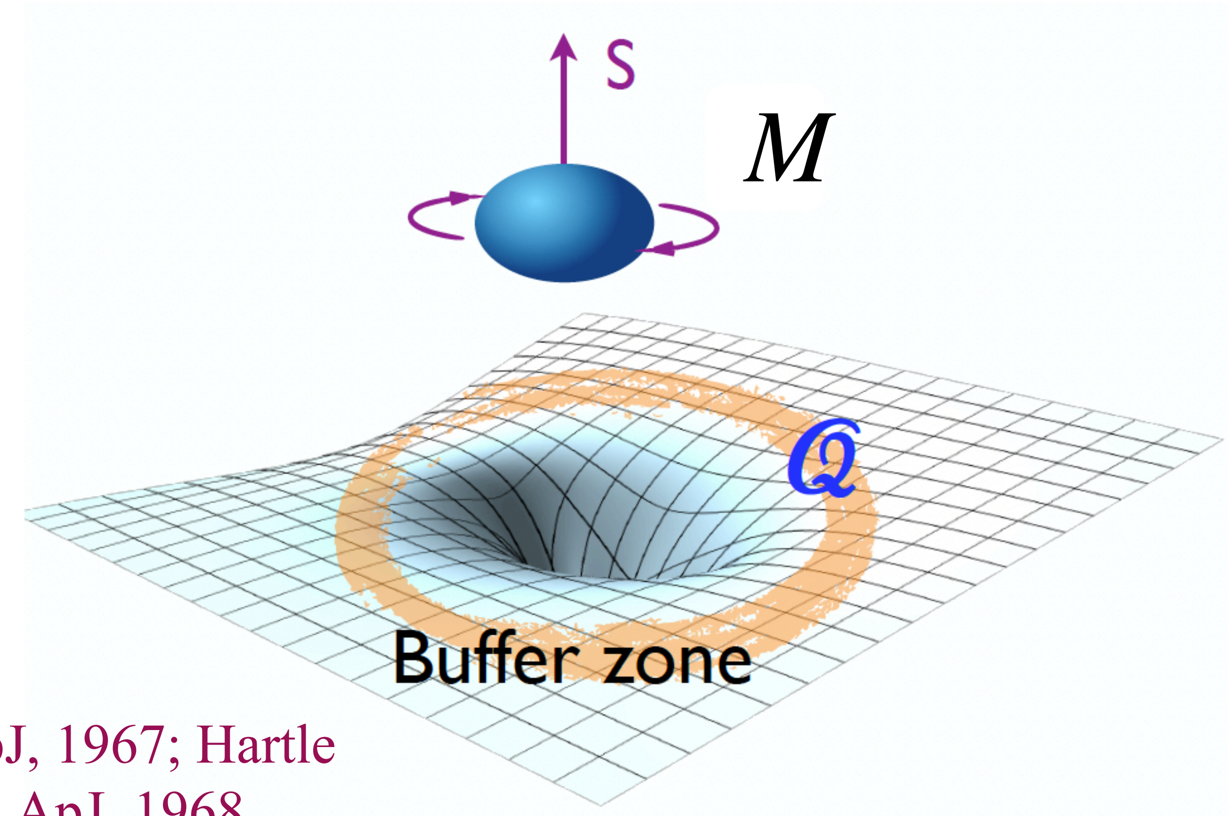

$$S = I\Omega$$

Moment of Inertia (MoI), $\propto R^2$

$$Q = -\bar{Q}\,\chi^2 M^3$$

Dimensionless Quadrupole, $\propto \Omega^2 R^5$

Dimensionless spin parameter

Hartle, ApJ, 1967; Hartle & Thorne, ApJ, 1968

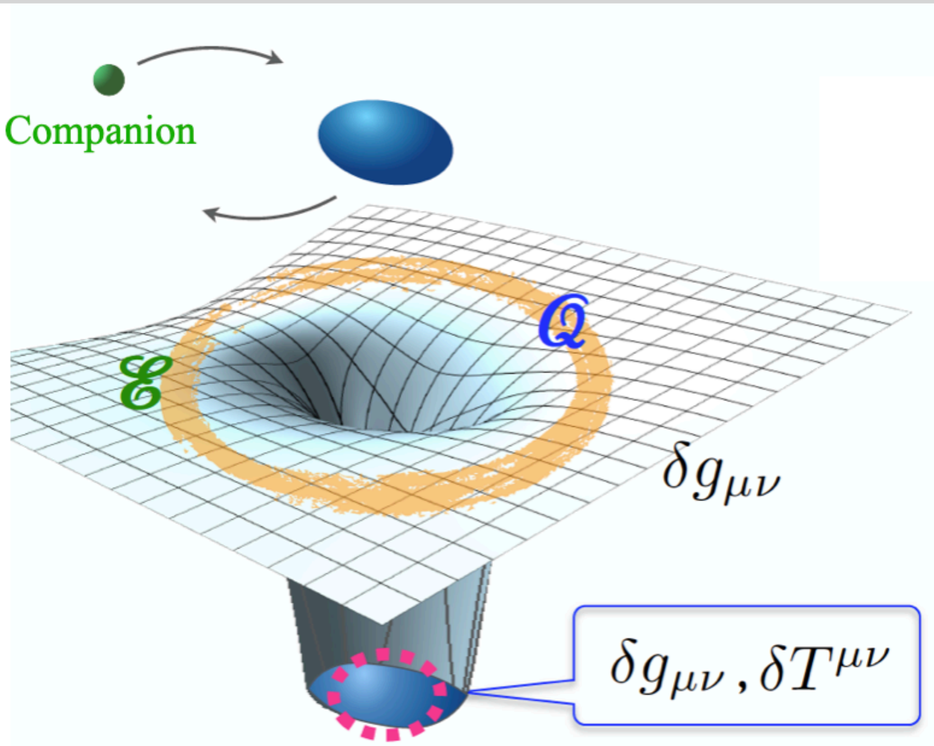

Credit: Tanja Hinderer

$$Q_{ij} = -\lambda \mathcal{E}_{ij} \qquad \lambda = \frac{2}{3} k_2 R^5$$

Tidal deformability, $\propto R^5$

Hinderer, ApJ, 2008; Hinderer & Flanangan, PRD, 2008; Damour & Nagar, PRD, 2009

Moment of inertia (MoI) measurements

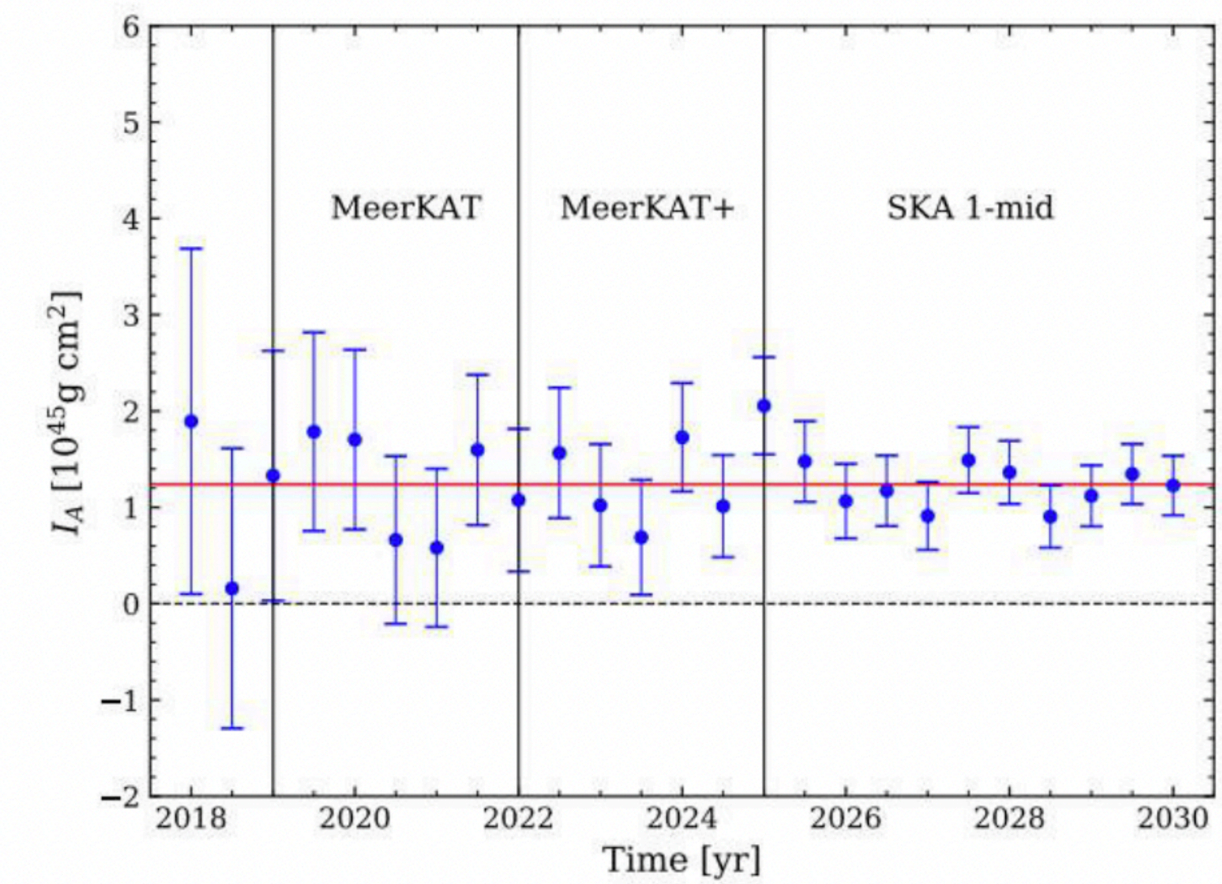

Measure MoI from Lense-Thirring precession

$$\dot{\omega}^{\rm intr} = \dot{\omega}^{\rm 1PN} + \dot{\omega}^{\rm 2PN} + \dot{\omega}^{\rm LT,A}$$
$$= \frac{3\beta_{\rm O}^2 n_{\rm b}}{1 - e_{\rm T}^2}\left[1 + f_{\rm O}\beta_{\rm O}^2 - g_{\rm S_A}^{\parallel}\beta_{\rm O}\beta_{\rm S_A}\right]$$

$$\beta_{\rm S_A} = \frac{cI_{\rm A}\Omega_{\rm A}}{Gm_{\rm A}^2}$$ MoI (EoS) dependent

Damour & Schaeffer, Nuovo Cimento B Serie, 1988

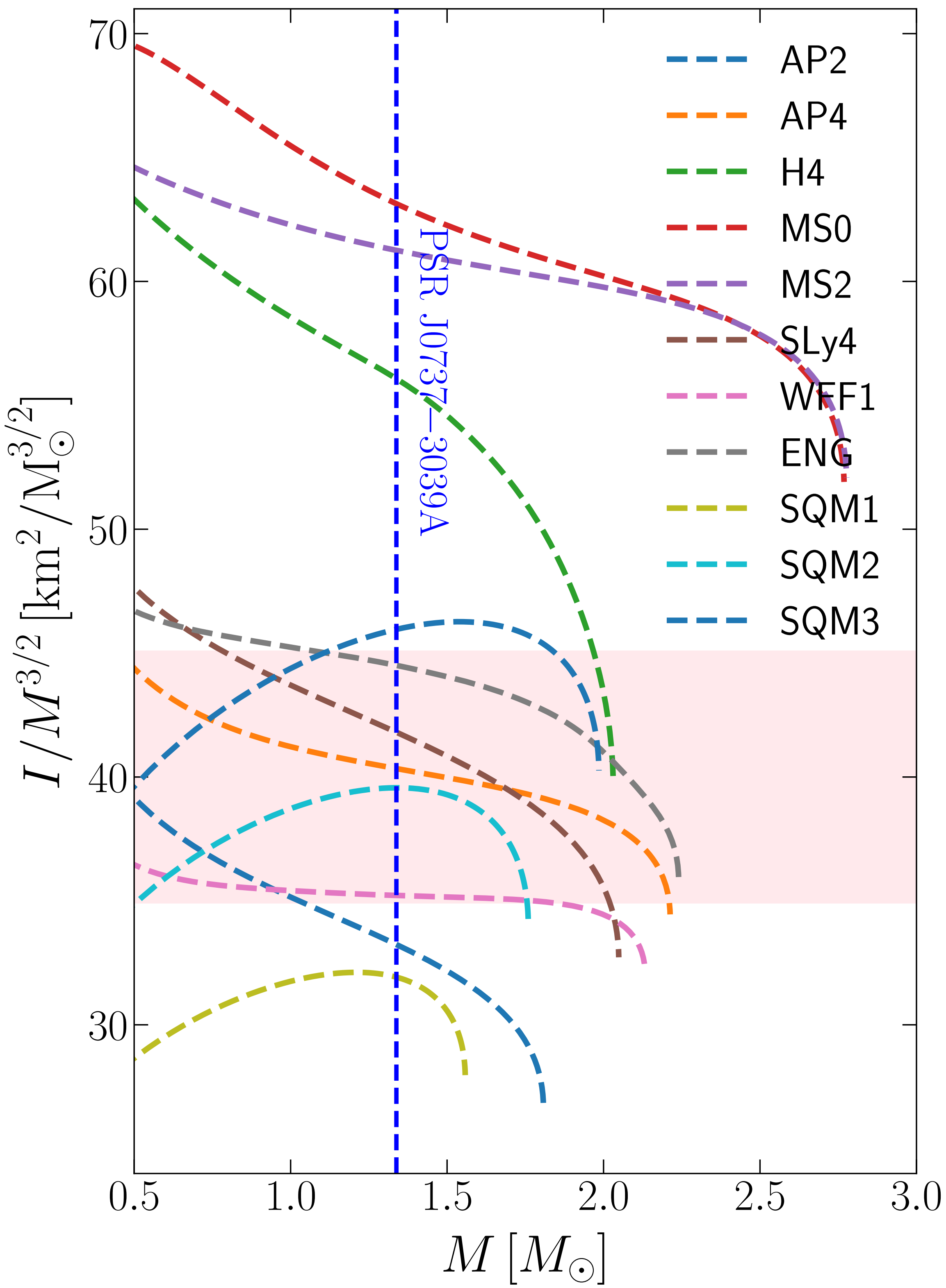

Gao et al., MNRAS, 2022

Tidal constraints from GW170817

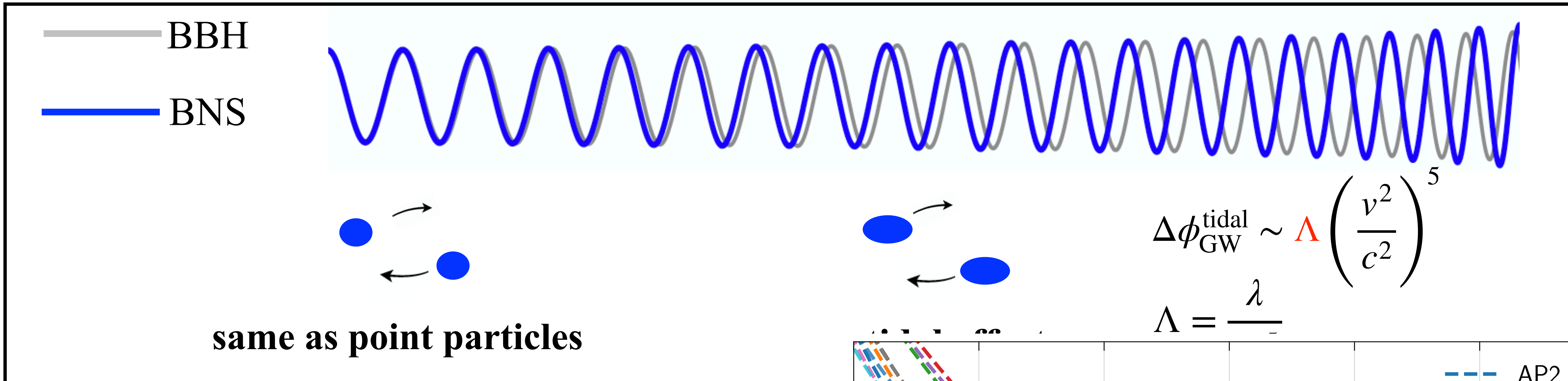

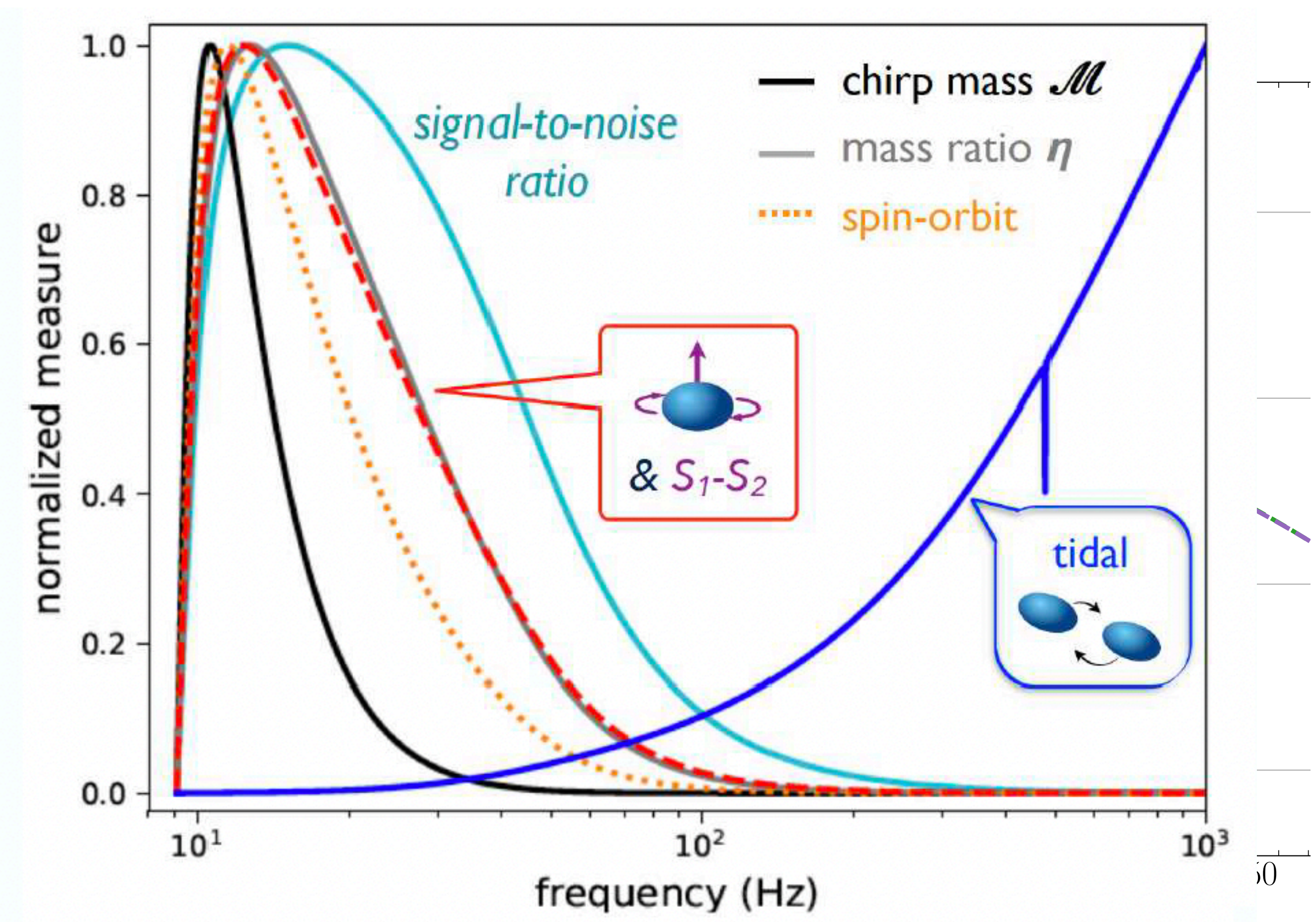

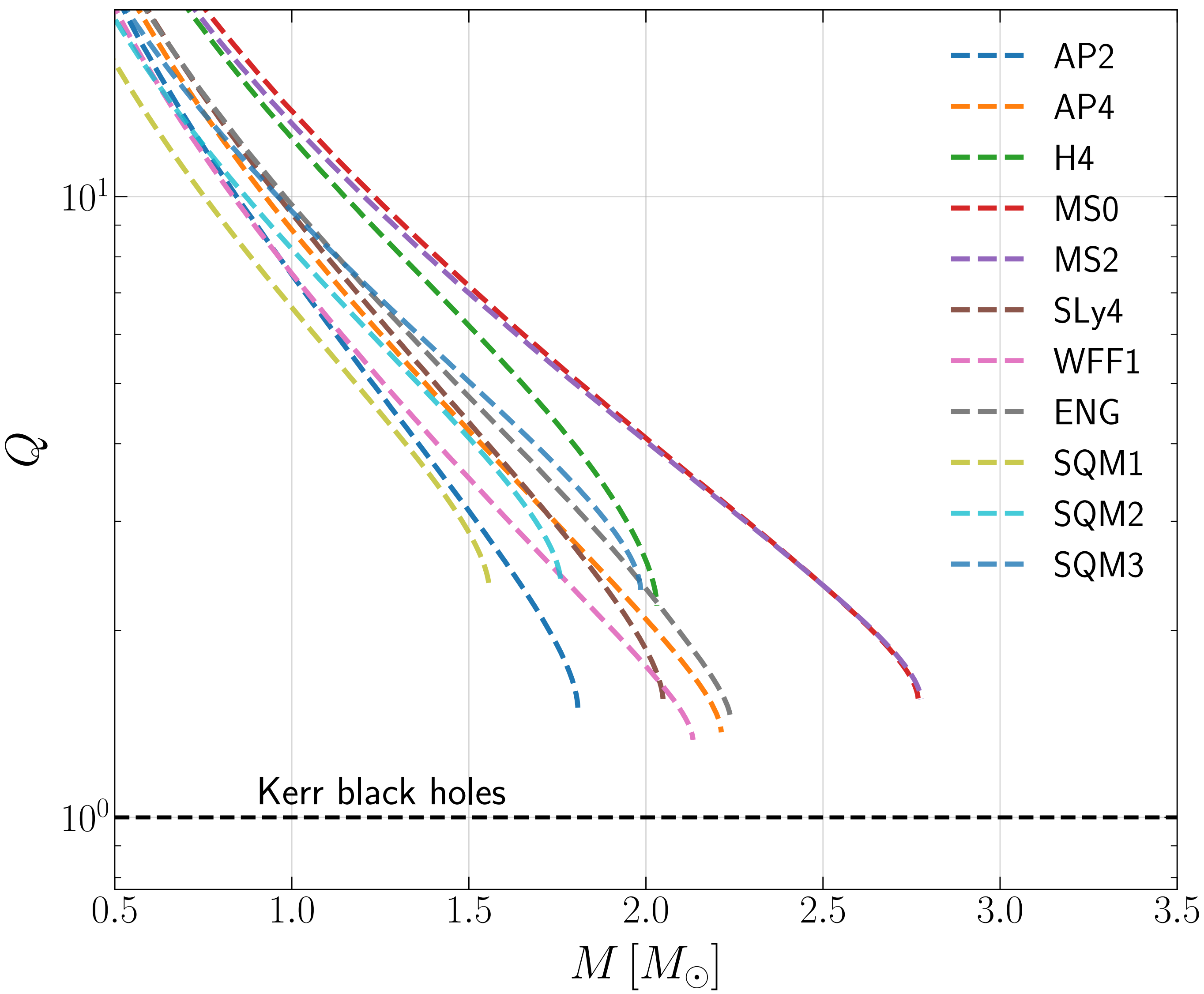

Abbott et al., PRL, 2017, 2019; Gao et al., MNRAS, 2022

Go beyond global properties

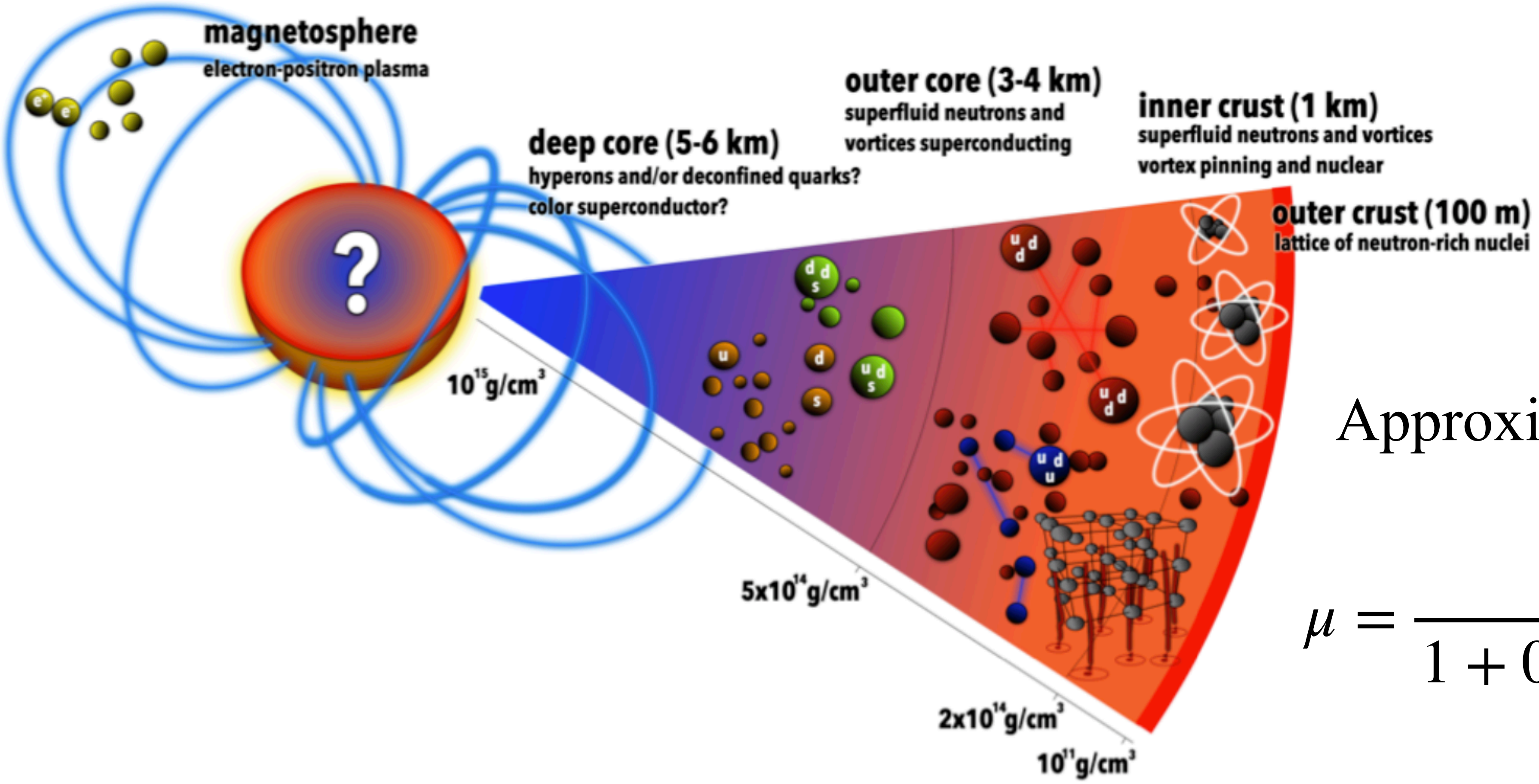

Approximately

$$\mu = \frac{0.1194}{1 + 0.595(173/\Gamma)^2} \frac{n_i (Ze)^2}{a}$$

Solid components, elasticity, $\mu \sim 10^{29} - 10^{30}\,\mathrm{erg\,cm^{-3}}$

Superfluidity: Fermi surface phenomenon, important for pulsar glitch

QCD phase transition: dynamics of BNS inspiral/merger and CCSN, maybe more?

Non-hydro deformations: mountains

$$\epsilon = \frac{I_3 - I_0}{I_0}$$

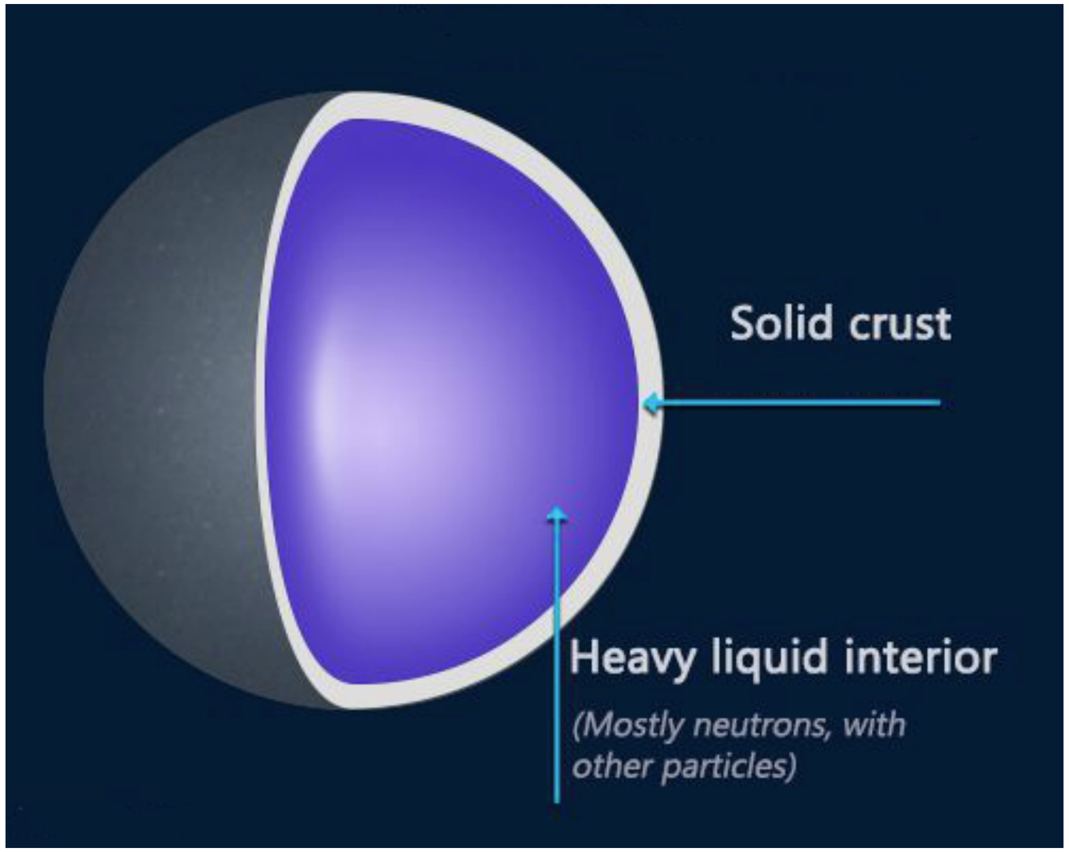

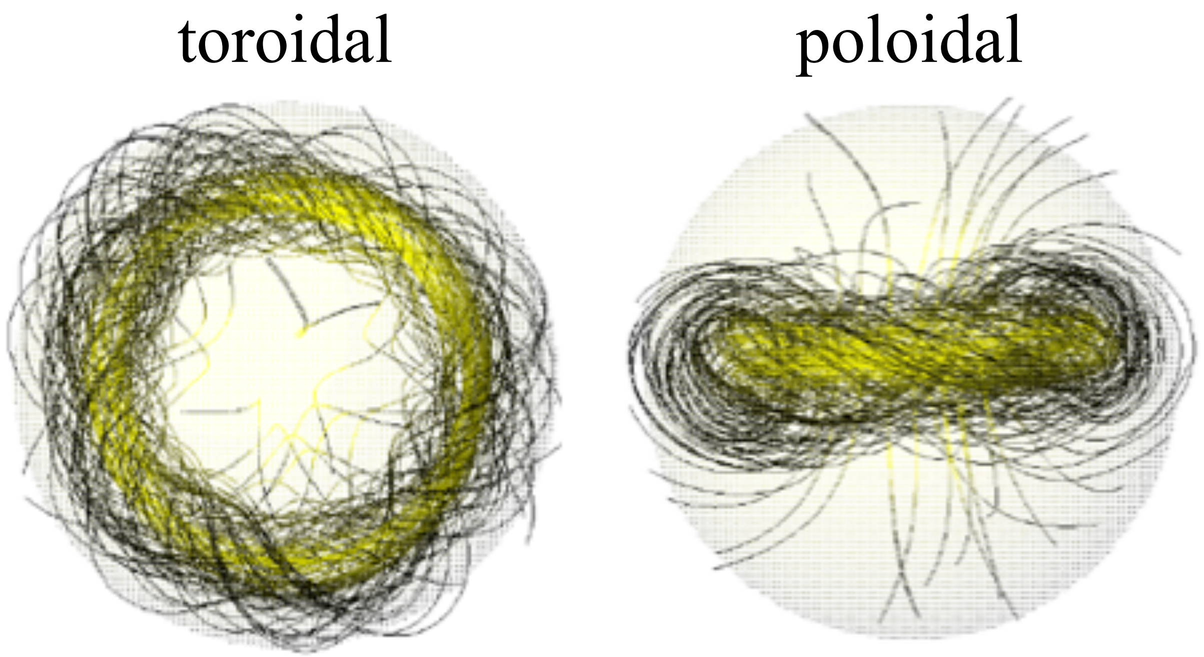

Credit: Braithwaite

$$\epsilon_c = bu = 10^{-6}\left(\frac{b}{10^{-6}}\right)\left(\frac{\sigma_{\rm break}}{10^{-1}}\right)$$

Cutler et al., PRD, 2003; Gittins et al., MNRAS, 2021

$$\epsilon_B \approx \kappa \frac{B^2 R^3}{GM^2/R} = 1.9 \times 10^{-6} \kappa B_{15}^2$$

Lander & Jones, MNRAS, 2009; Lasky & Melatos, PRD, 2014; Zanazzi & Lai, MNRAS, 2015

- Important information on NS crust physics: shear modulus & breaking strain
- Information on NS internal magnetic field configuration and strength

Non-hydro deformations: mountains

$$\epsilon = \frac{I_3 - I_0}{I_0} \qquad h \approx 8 \times 10^{-28} \left(\frac{\epsilon}{10^{-6}}\right) \left(\frac{f}{100\ \mathrm{Hz}}\right)^2 \left(\frac{10\mathrm{kpc}}{d}\right)$$

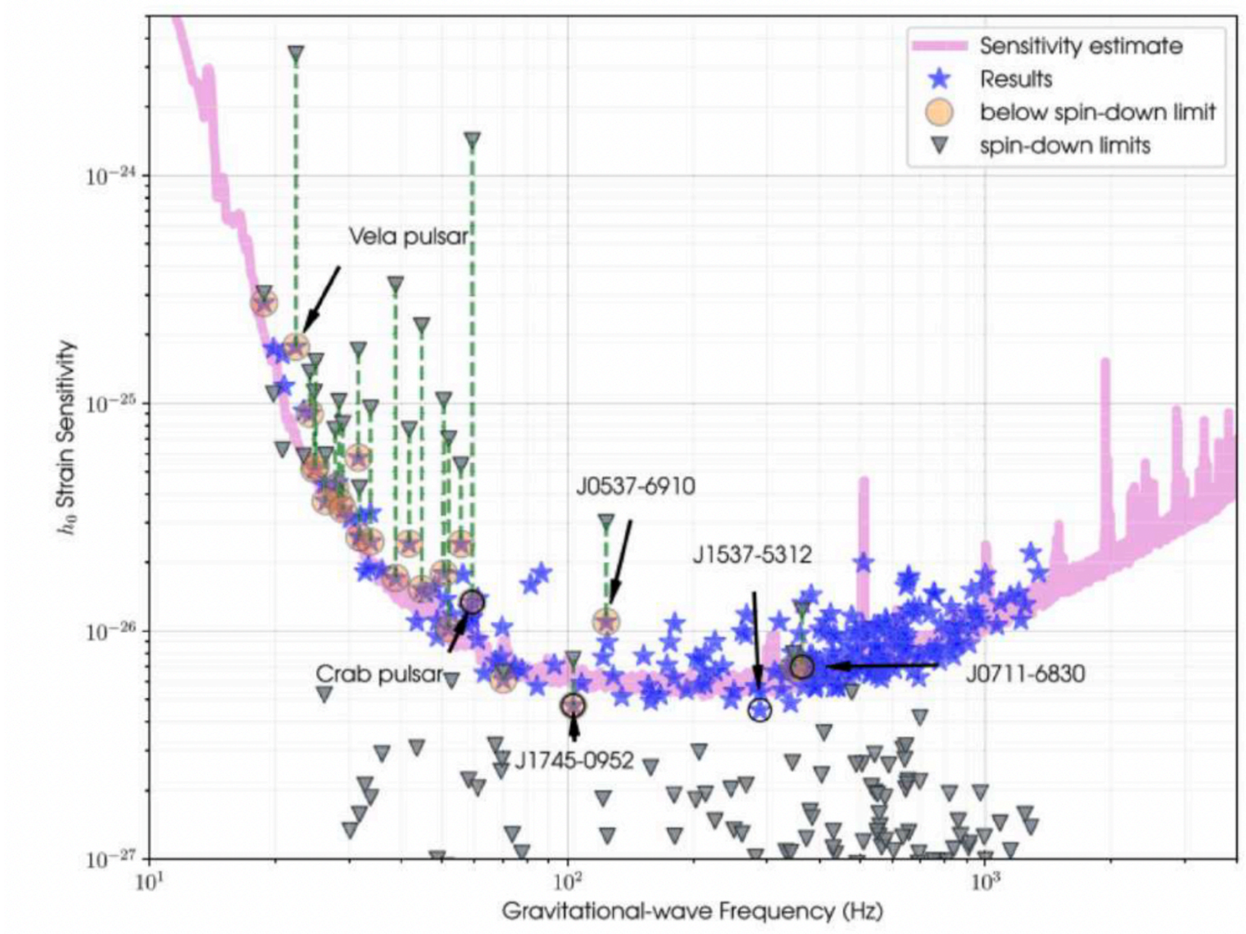

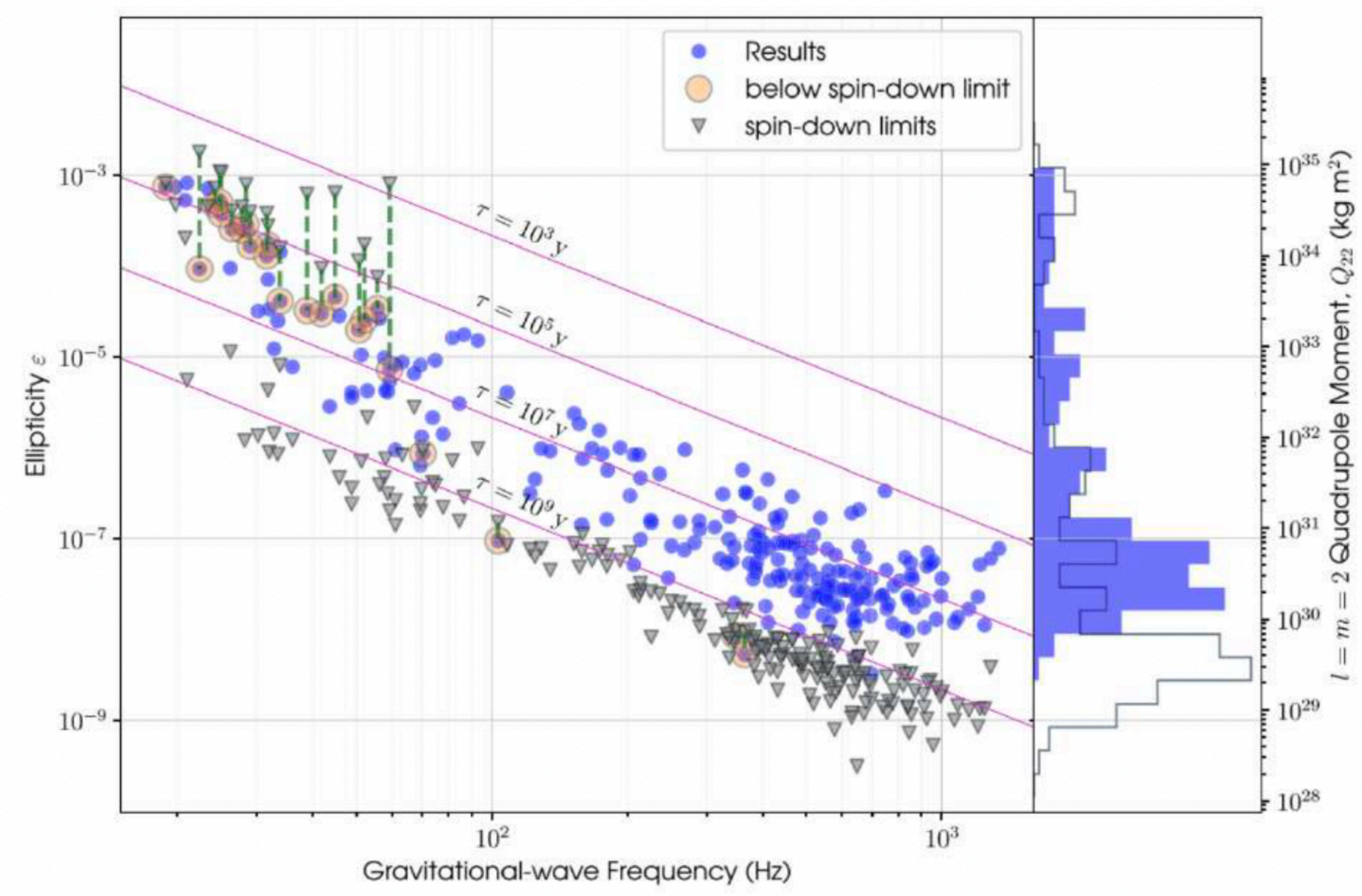

Free precession of NSs

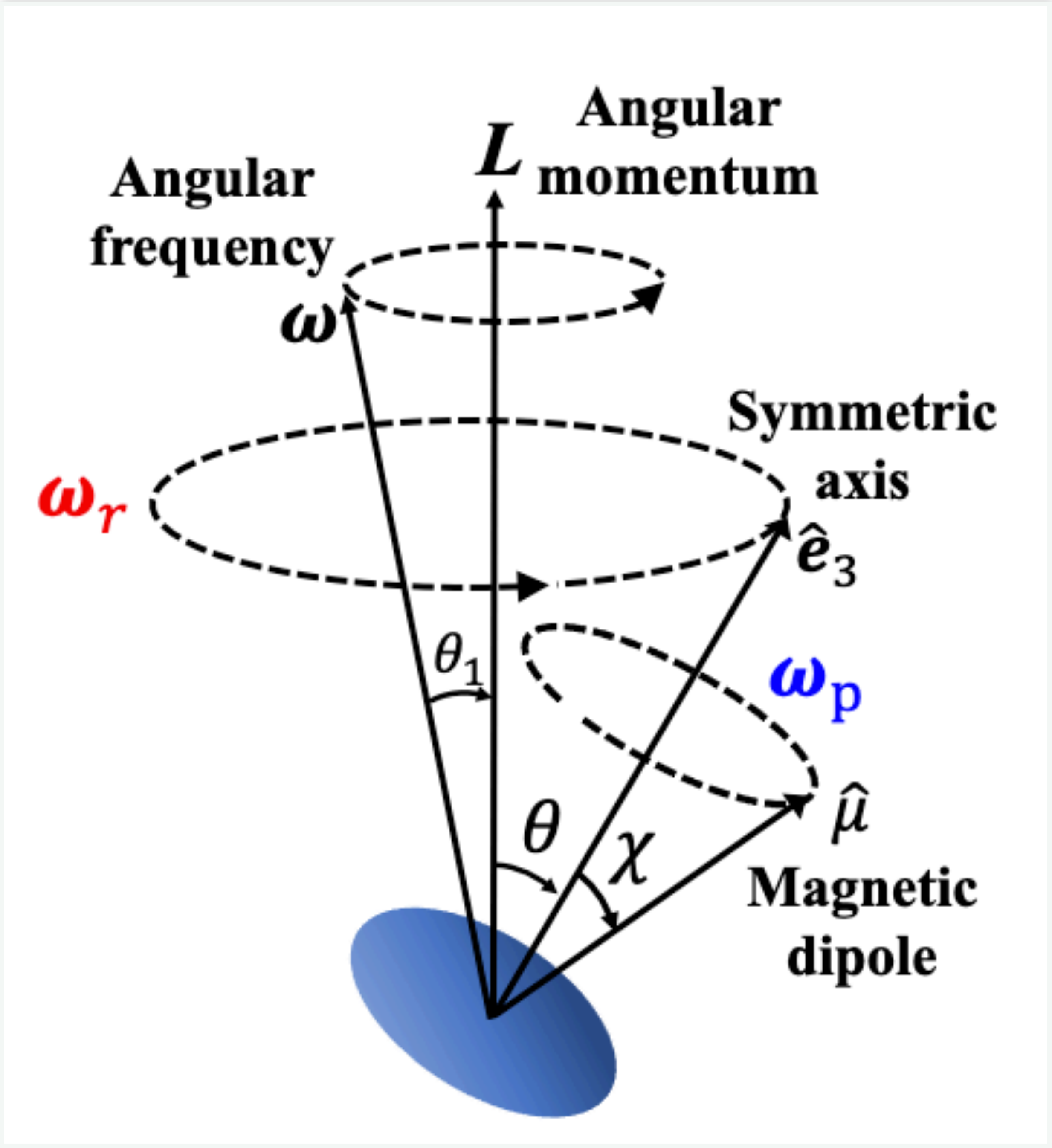

Free precession of a biaxial star

Jones & Andersson, MNRAS, 2001, 2002
Link & Epstein, ApJ, 2001

- Precession happens if some deformation pieces are not aligned with the rotation bulges

ellipticity $\epsilon = \dfrac{\Delta I_\mathrm{d}}{I_0}$ wobble angle: θ

- The ellipticity for NSs is quite small

$\epsilon \ll 10^{-4}$ from current calculations

$\theta_1 \sim \epsilon\theta$, $\boldsymbol{\omega}$ and $\boldsymbol{L}$ are nearly aligned

- **Two superimposed motion:**

$$\boldsymbol{\omega} = \omega_\mathrm{r}\hat{\boldsymbol{L}} - \omega_\mathrm{p}\hat{\boldsymbol{e}}_3 \qquad \omega_\mathrm{p} = \epsilon\cos\theta\,\omega_\mathrm{r}$$

Precession period $P_\mathrm{f} = \dfrac{P}{\epsilon\cos\theta}$

Precession of NSs

Superfluid does not support long precession period without damping

- A **perfectly pinned** superfluid, the Euler equation

$$\dot{\boldsymbol{L}}_\mathrm{c} + \boldsymbol{\omega} \times \boldsymbol{L}_\mathrm{c} = -\boldsymbol{\omega} \times \boldsymbol{L}_\mathrm{f} \longrightarrow \omega_\mathrm{p} \sim -\left(\epsilon + \frac{I_\mathrm{f}}{I_\mathrm{c}}\right)\omega$$

Pinning gives a precession frequency too fast!

- "Mutual friction" between superfluid and crust leads to **damping of free precession**

$$\frac{\mathrm{d}\boldsymbol{J}_\mathrm{shell}}{\mathrm{d}t} = K\left(\boldsymbol{\Omega}_\mathrm{fluid} - \boldsymbol{\Omega}_\mathrm{solid}\right) = -\frac{\mathrm{d}\boldsymbol{J}_\mathrm{fluid}}{\mathrm{d}t}$$

- Challenge our current understanding of superfluid state in NS interior

Possible evidence

Stairs et al., Nature, 2000; Link & Epstein, ApJ, 2001

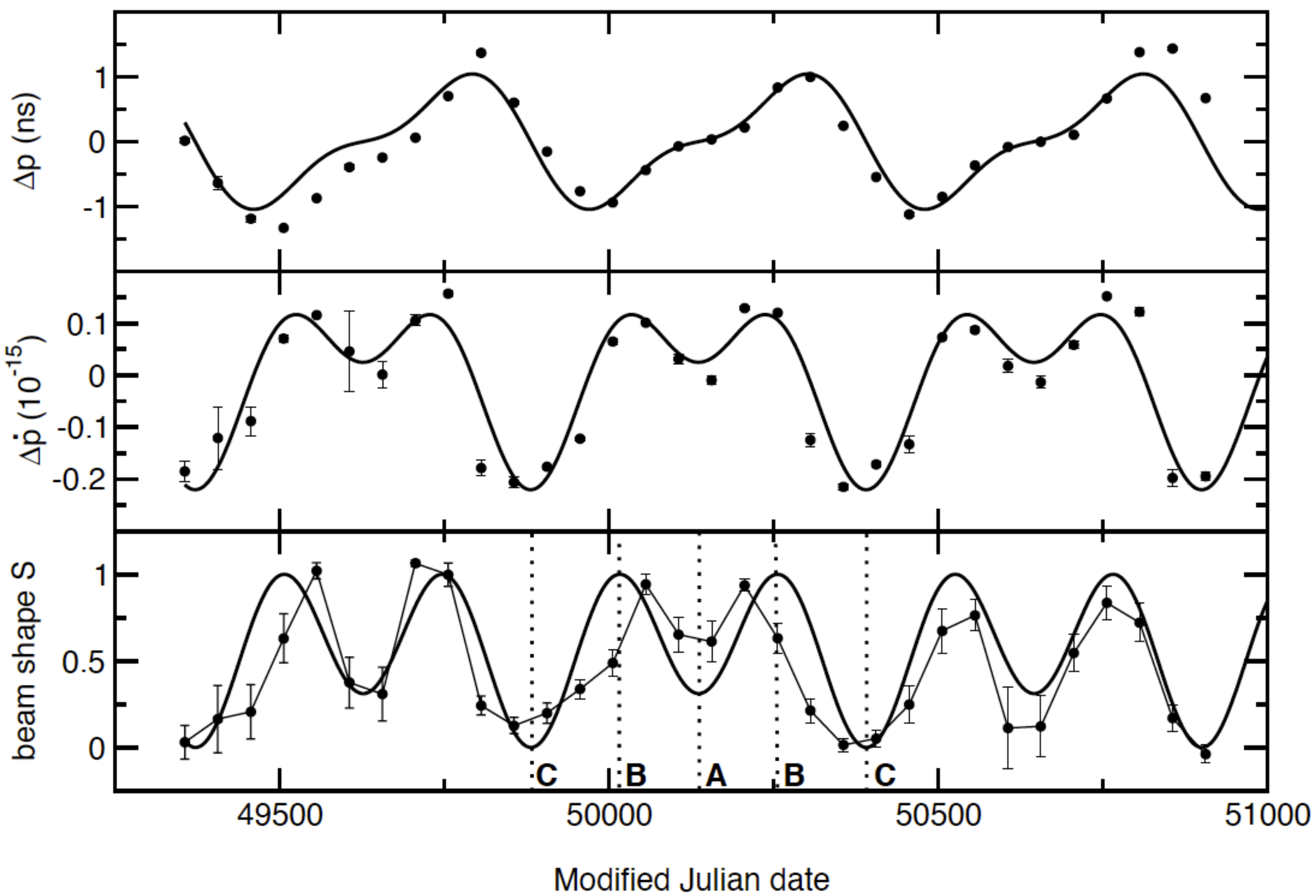

PSR B1828-11: radio timing and beam shape

$P_{\rm f} \sim 500\,\text{days} \qquad \epsilon \sim 10^{-8}$

Makishima et al., PRL, 2014

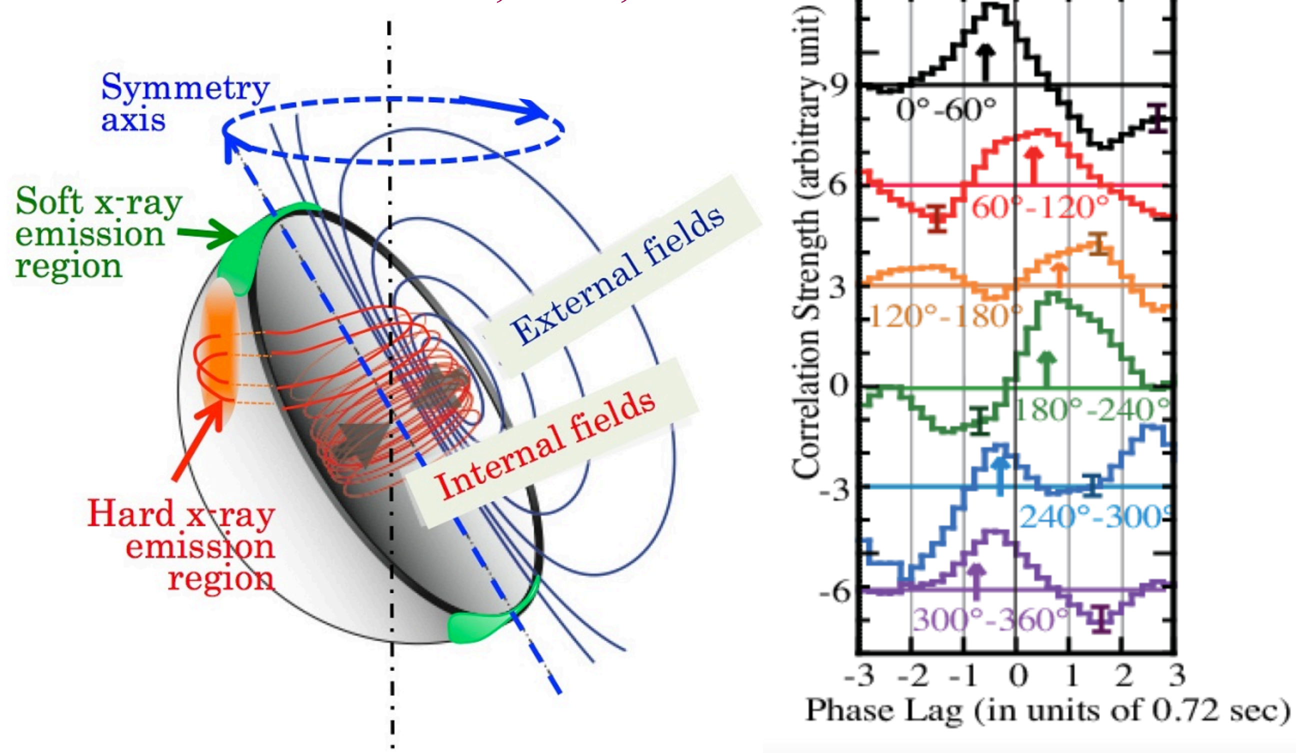

Magnetar 4U 0142+61: hard X-ray phase modulations (±0.7 s)

$P_{\rm f} \sim 15\,\text{h} \qquad \epsilon \sim 10^{-4}\,!$

Indication of strong internal toroidal magnetic field in the order of 10^{16} G

Precession of magnetars: dynamics

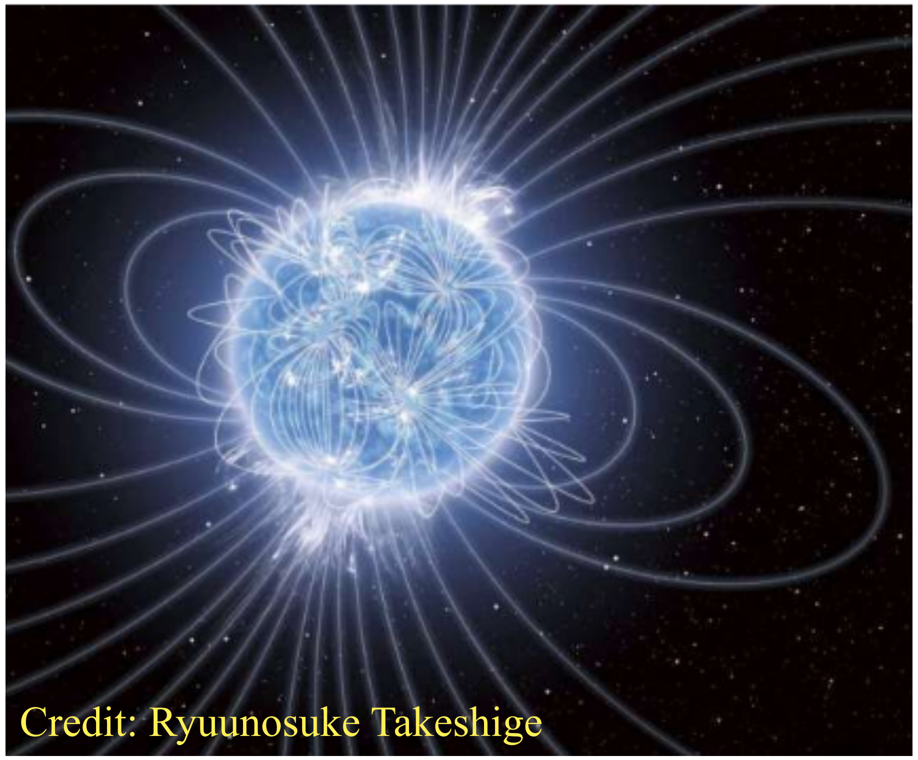

- Internal magnetic fields are complex, multipoles
- Possible elastic deformation + magnetic deformation

- Large deformation due to strong internal magnetic field
$$\epsilon_{\rm B} \approx \kappa \frac{B^2 R^3}{GM^2/R} = 1.9 \times 10^{-6} \kappa B_{15}^2$$
- They are young and very active, energetic process may excite wobble angle and precession

Levin et al., ApJ, 2020

We need solution for triaxial stars

$$\dot{\boldsymbol{L}} + \boldsymbol{\omega} \times \boldsymbol{L} = 0$$

$$\epsilon \equiv \frac{I_3 - I_1}{I_1}, \quad \delta \equiv \frac{I_3\left(I_2 - I_1\right)}{I_1\left(I_3 - I_2\right)}, \quad \theta \equiv \arccos \frac{L_3}{L}$$

- Precession + Rotation + **Nutation**
- The solutions are **not harmonic**, can be represented by **Jacobi elliptic functions**

Landau & Lifshitz, Mechanics, 1960

Precession of magnetars: dynamics

- Large magnetic field indicates large electromagnetic torques

The near-field torque

$$N_{\mathrm{m}} = \frac{3\omega^2\mu^2}{5Rc^2}(\hat{\boldsymbol{\omega}} \cdot \hat{\boldsymbol{\mu}})(\hat{\boldsymbol{\omega}} \times \hat{\boldsymbol{\mu}})$$

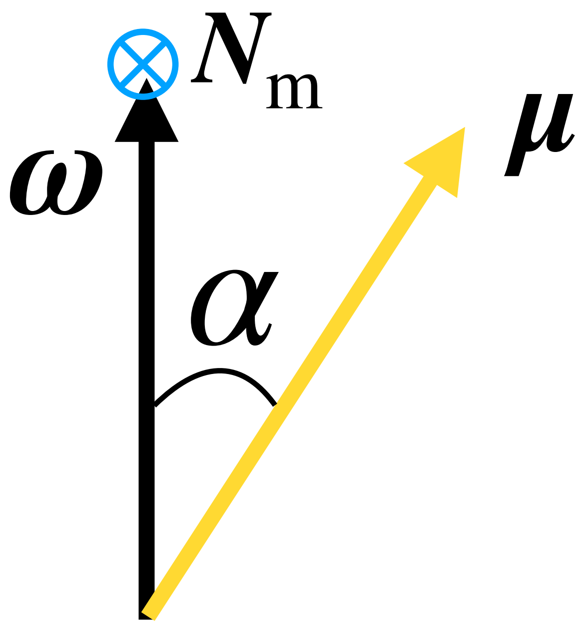

Does not dissipate energy, but changes the geometry

The far-field torque (spindown torque)

$$N_{\mathrm{rad}} = \frac{k_1\mu^2\omega^3}{c^3}\left[(\hat{\boldsymbol{\omega}} \cdot \hat{\boldsymbol{\mu}})\hat{\boldsymbol{\mu}} - k_2\hat{\boldsymbol{\omega}}\right]$$

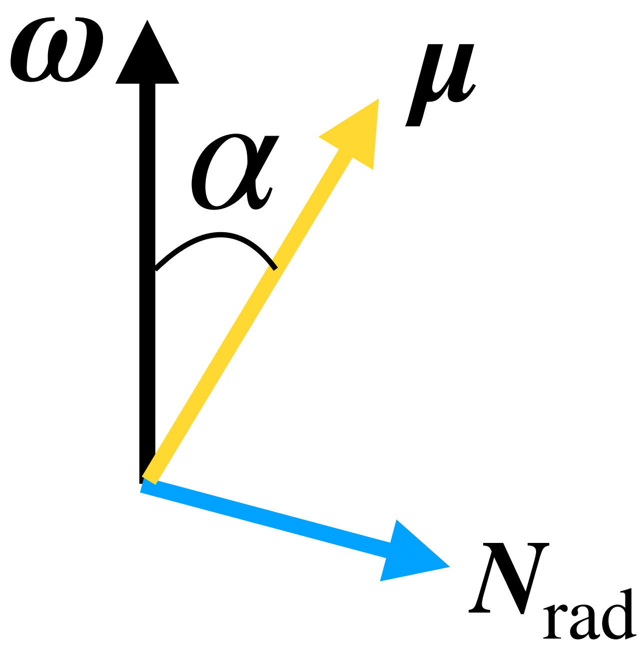

Dissipates energy (spindown) and changes the geometry

Goldreich, ApJ, 1970; Melatos, MNRAS, 2000; Beskin & Zheltoukhov, Phys. Usp. 2014; Zanazzi & Lai, MNRAS, 2015

Precession of magnetars: dynamics

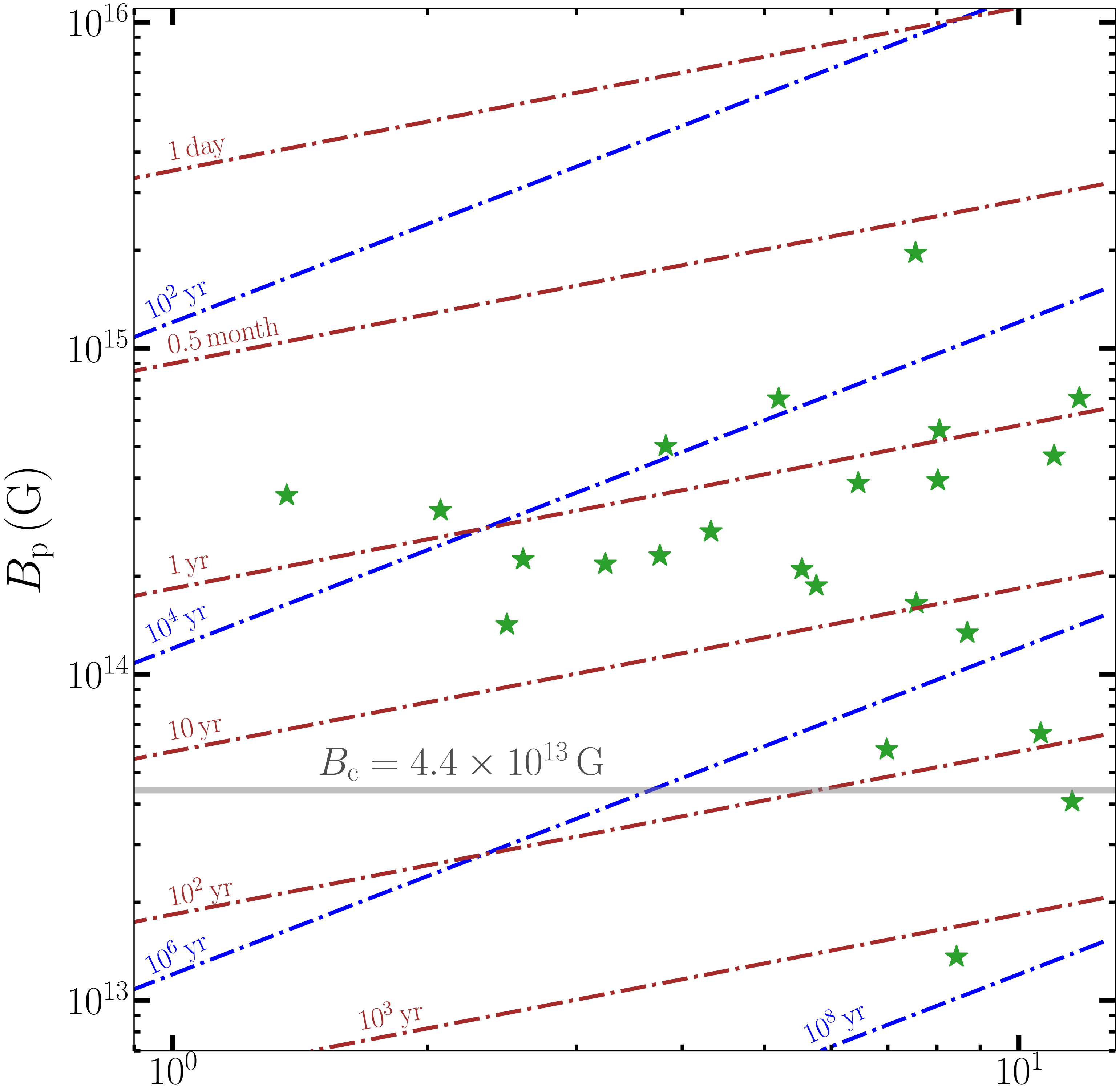

Gao et al., MNRAS, 2023

$$\tau_f \sim \frac{P}{\epsilon} = 1.58 P_5 \epsilon_7^{-1}\,\mathrm{yr}$$

$$\tau_f\,,\,\tau_m \ll \tau_{rad}$$

- Far-field torque can be obtained by perturbation method
- τ_m can be in the same order of τ_f, can be absorbed into the moment of inertia tensor of the star

We give **fully analytical** solution of forced precession

Timing residual

Gao et al., MNRAS, 2023

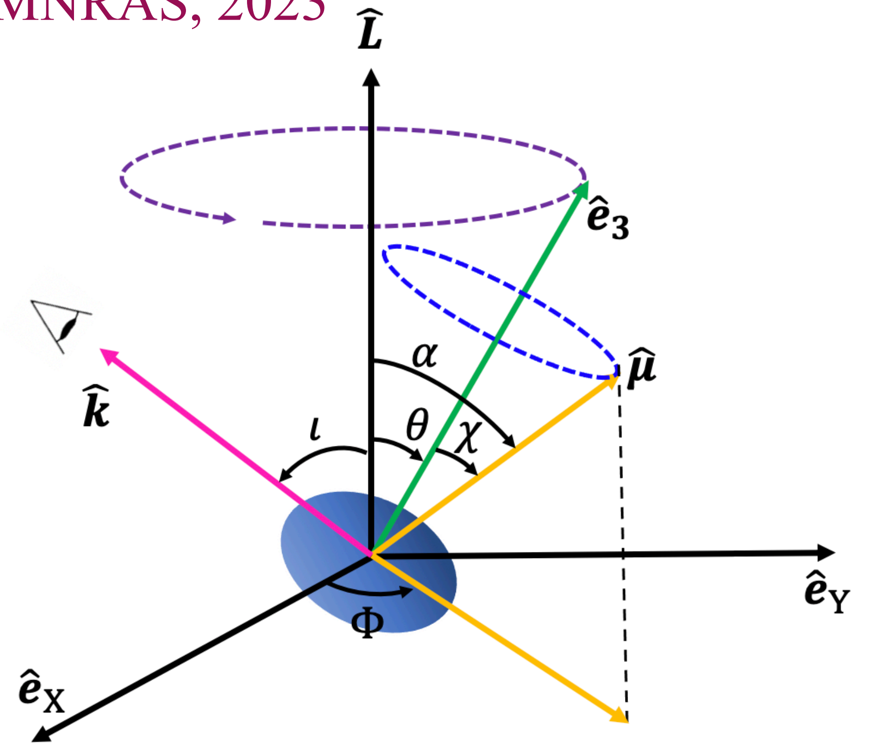

Spindown term dominates ($\epsilon = 10^{-7}$)

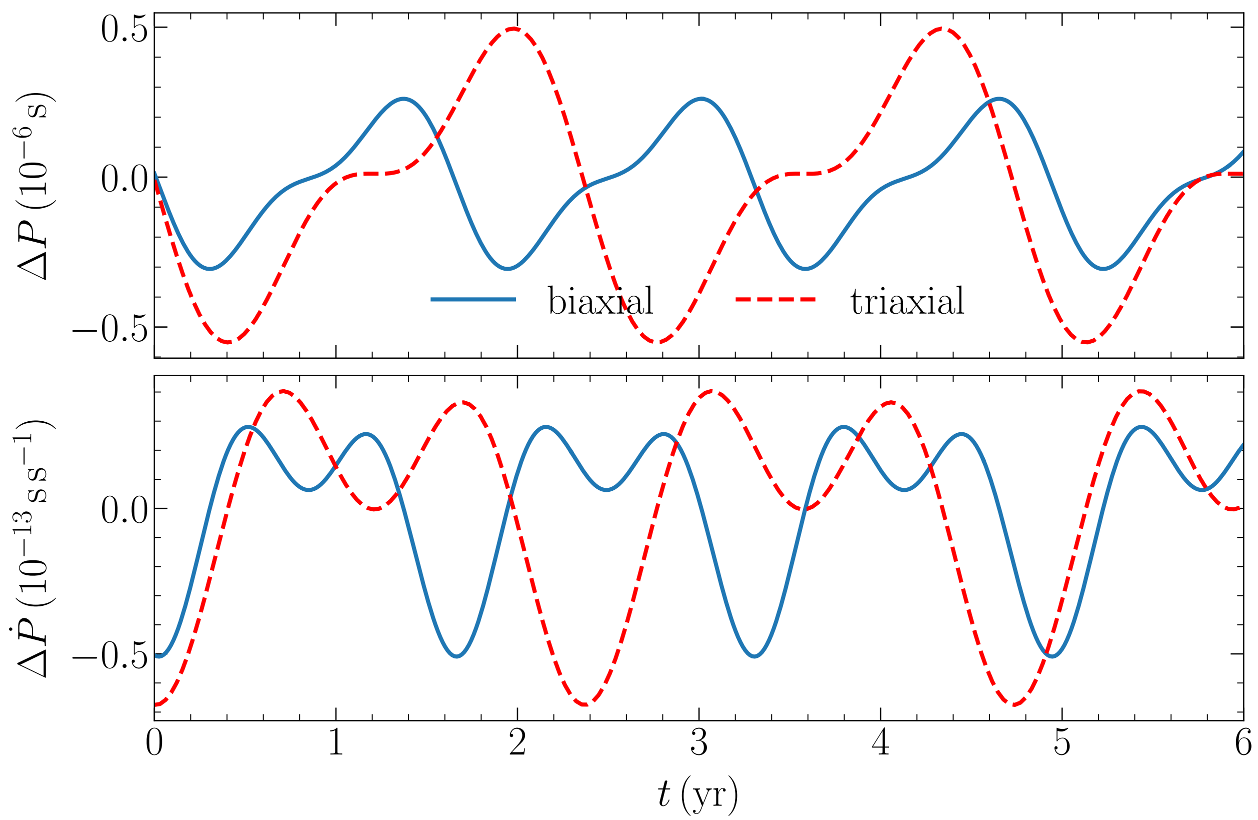

- The rotation phase Φ is different in different precession epoch

Geometric term dominates ($\epsilon = 10^{-4}$)

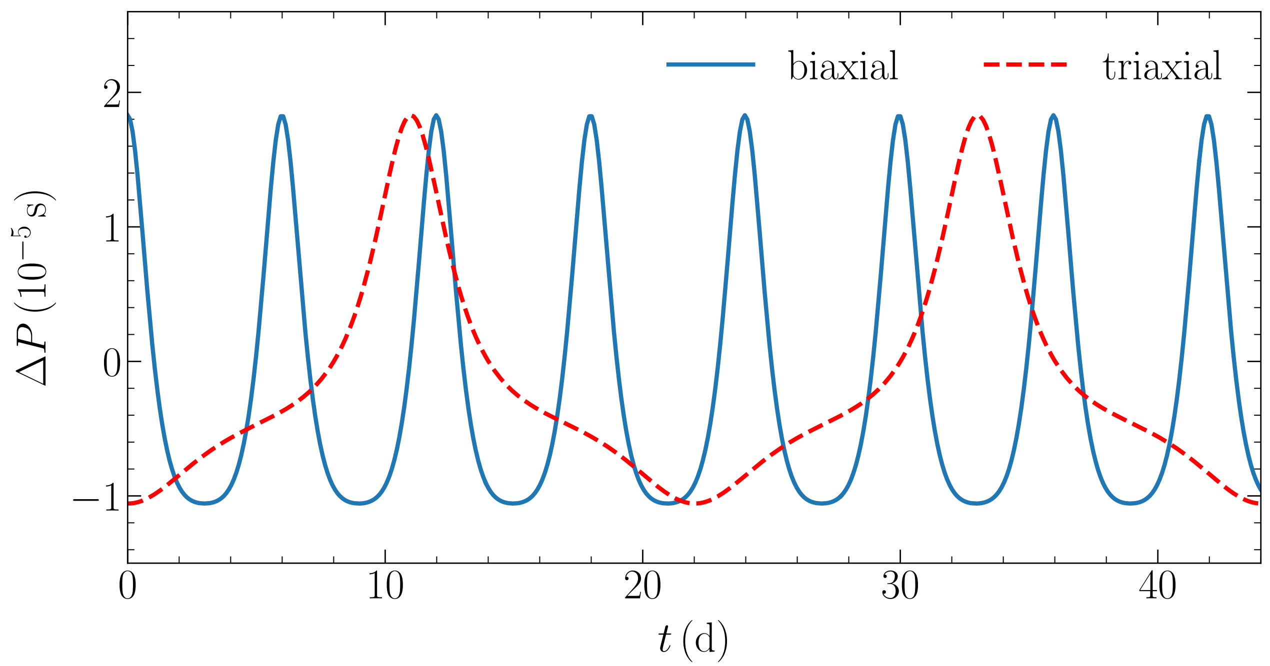

Phase modulations and timing residuals

$$\frac{\Delta P_{\rm fp}}{P} = \text{Geometric factor} \times \frac{P}{\tau_{\rm f}}$$

$$\frac{\Delta P_{\rm sd}}{P} = \text{Geometric factor} \times \frac{\tau_{\rm f}}{\tau_{\rm rad}}$$

Modulations on polarized electromagnetic waves

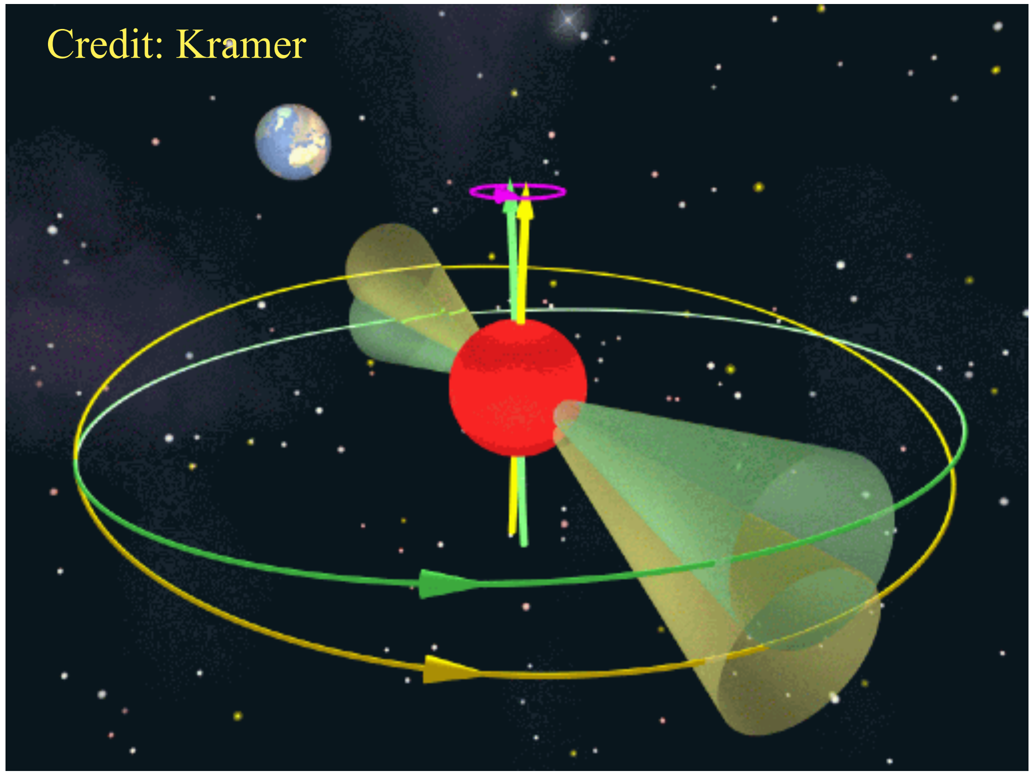

- The angle α changes periodically with precession period P_{f}

Swing of the emission region

Modulate flux, profile, **polarization**,…

Modulations on polarized radio emission

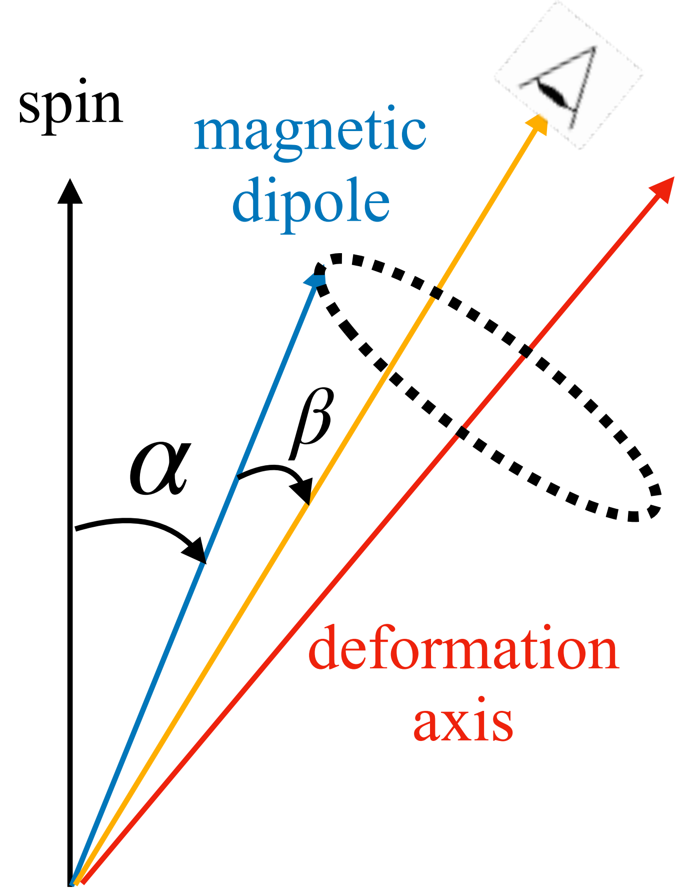

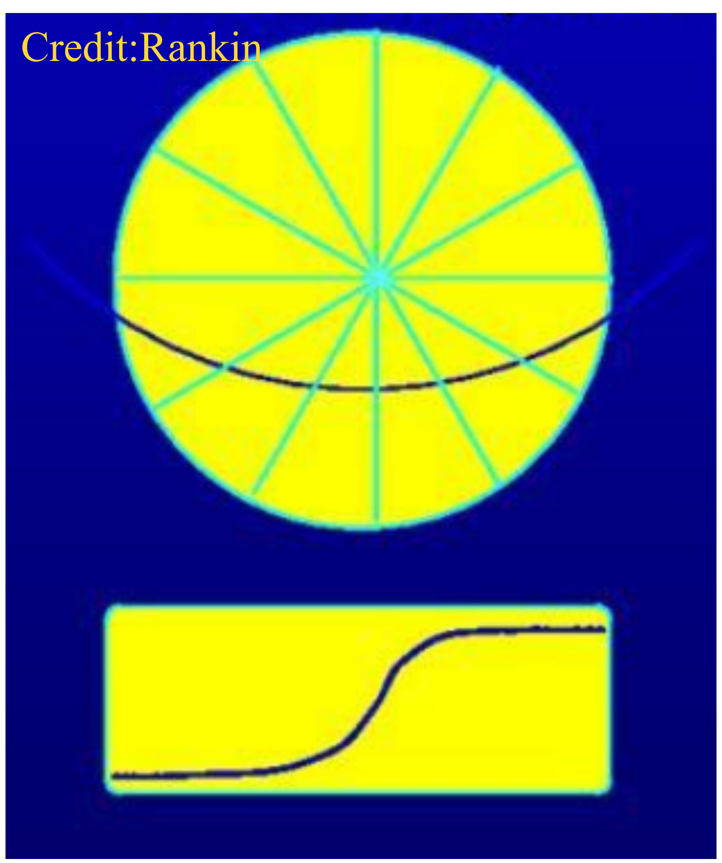

- Radio emission detected in transient magnetars, highly linearly polarized (60%-100%)

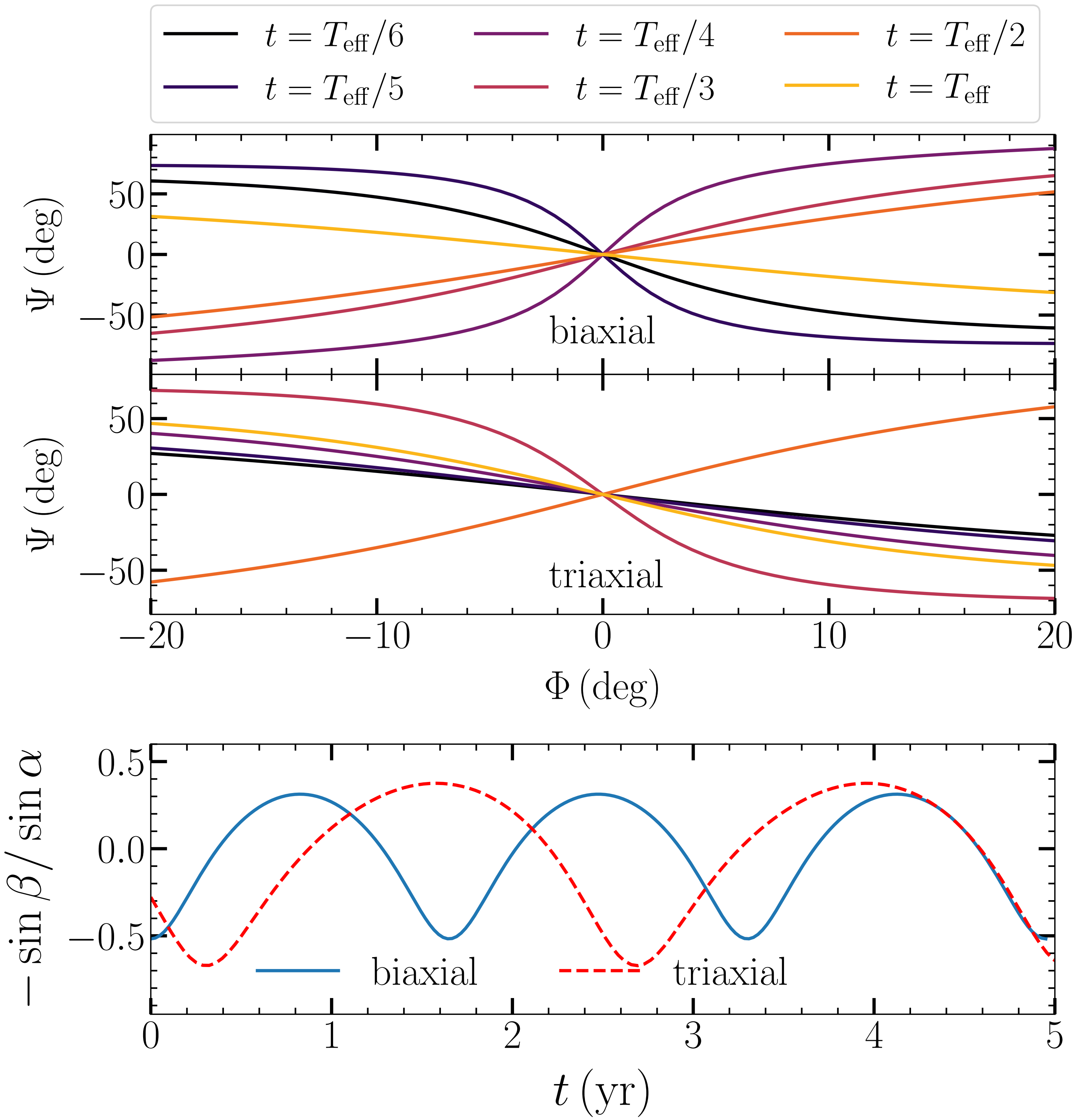

A freely precessing magnetar after X-ray burst

XTE J1810-197, obtained from radio polarization

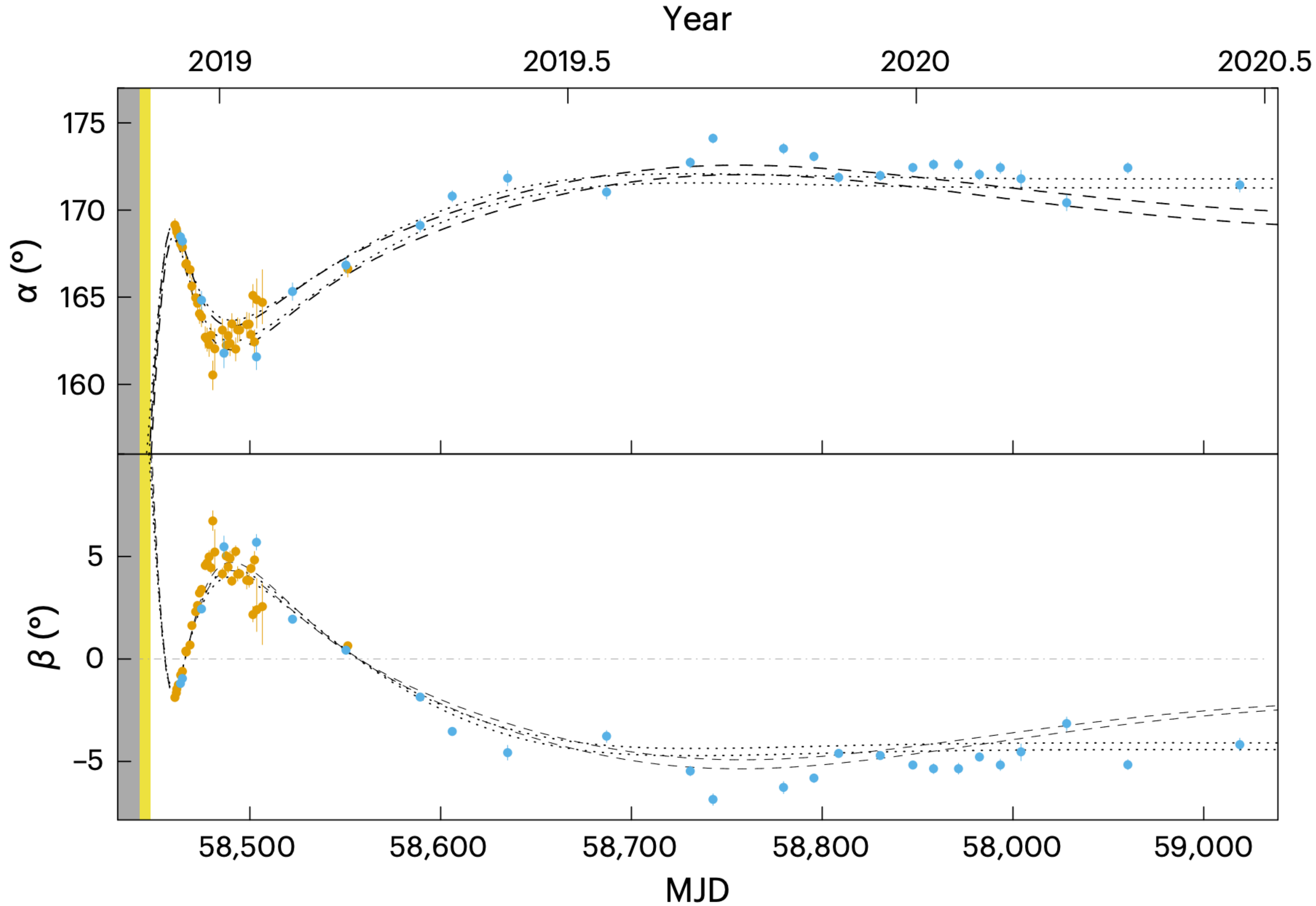

Desvignes et al., Nature Astronomy, 2024

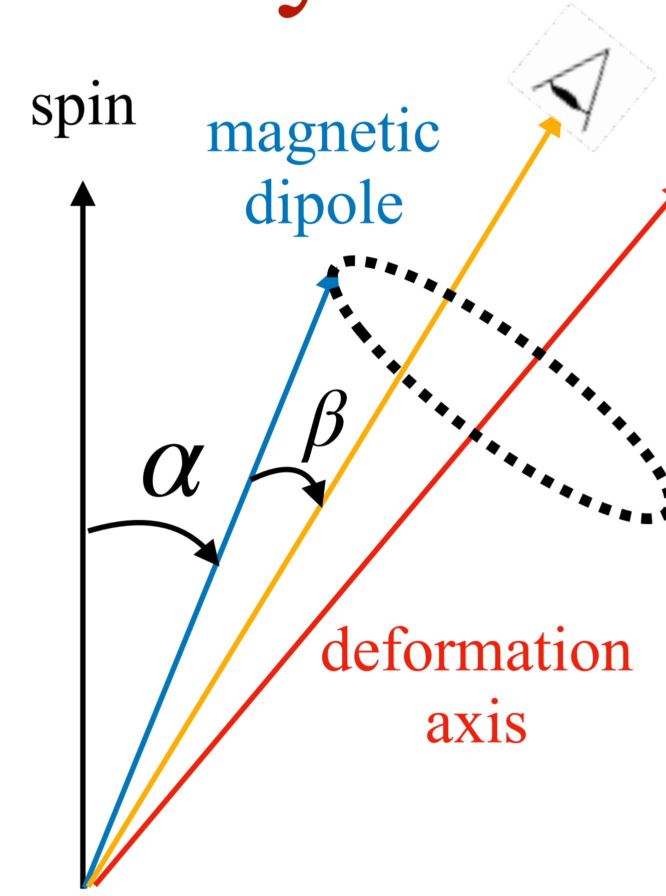

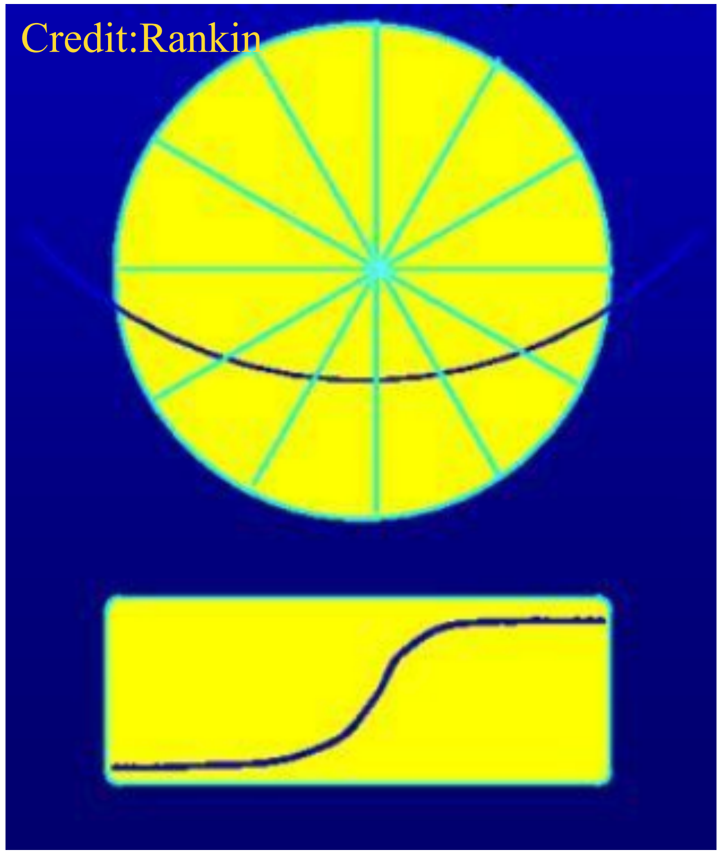

A freely precessing magnetar after X-ray burst

XTE J1810-197, obtained from radio polarization

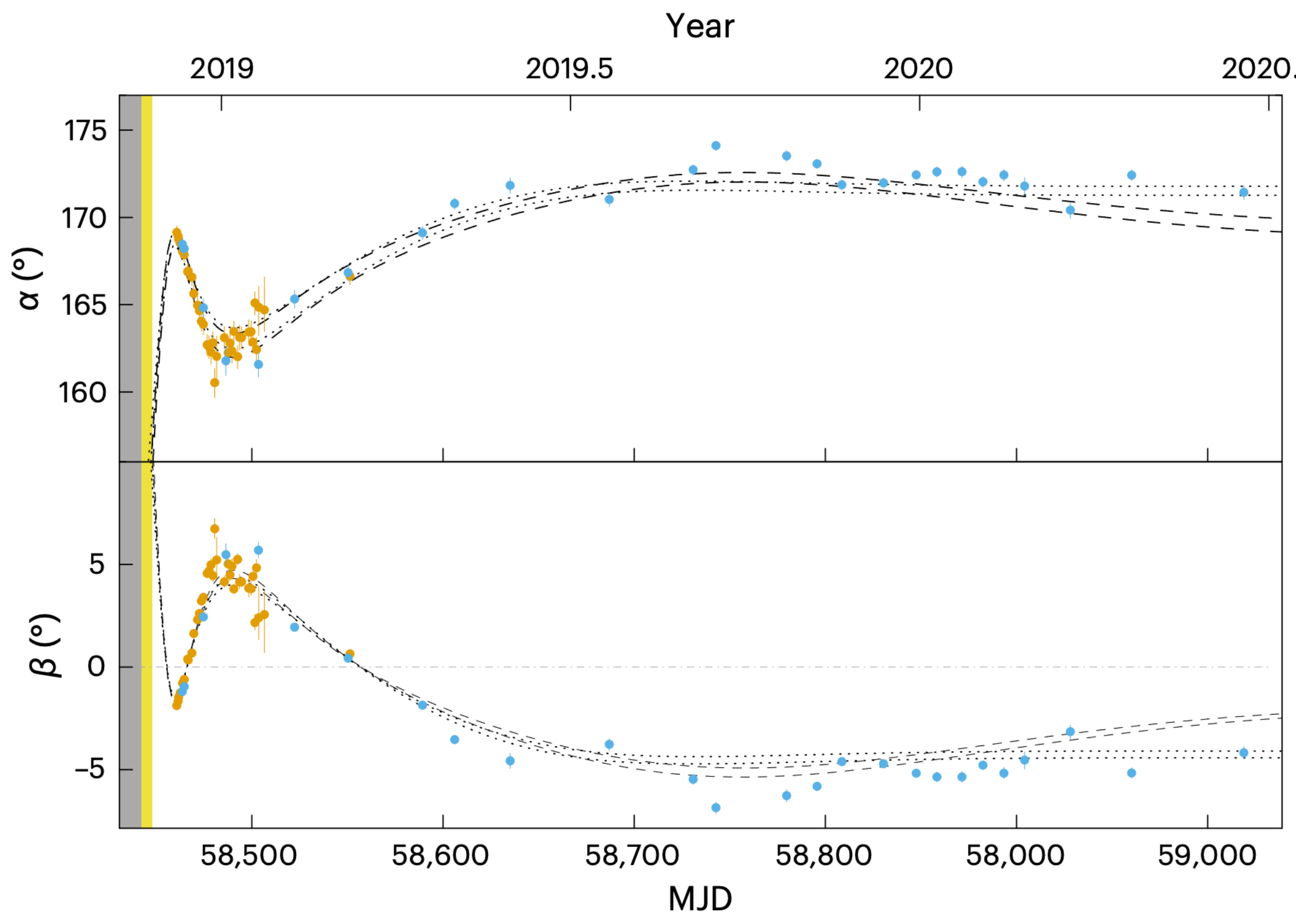

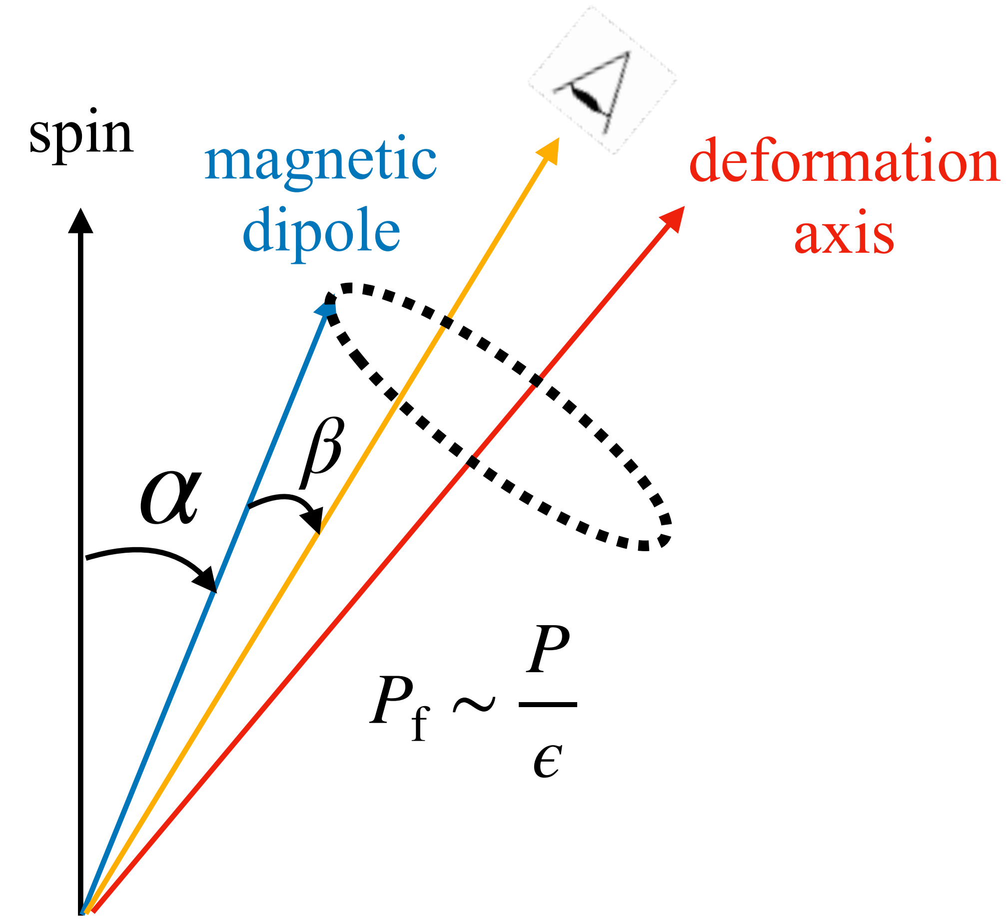

Desvignes et al., Nature Astronomy, 2024

1. Ellipticity decay model

$$P_{\mathrm{f}} \sim \frac{P}{\epsilon(t)}$$

2.Frictional coupling model

$$\dot{\boldsymbol{L}}_{\mathrm{c}} + \boldsymbol{\omega}_{\mathrm{c}} \times \boldsymbol{L}_{\mathrm{c}} = \boldsymbol{N}_{\mathrm{int}}$$

$$\dot{\boldsymbol{L}}_{\mathrm{f}} + \boldsymbol{\omega}_{\mathrm{c}} \times \boldsymbol{L}_{\mathrm{f}} = -\boldsymbol{N}_{\mathrm{int}}$$

$$\boldsymbol{N}_{\mathrm{int}} = K\left(\boldsymbol{\Omega}_{\mathrm{f}} - \boldsymbol{\omega}_{\mathrm{c}}\right)$$

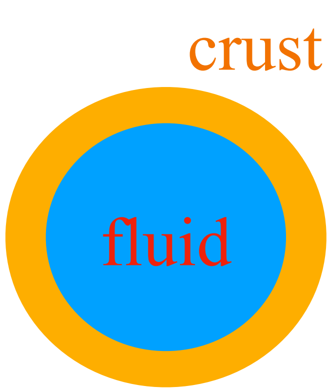

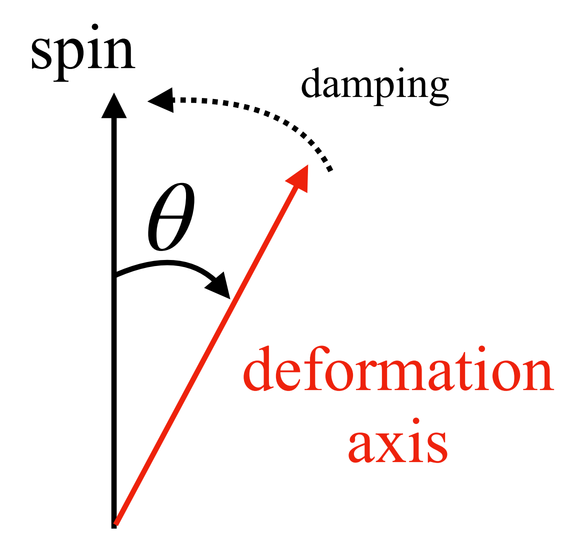

A freely precessing magnetar after X-ray burst

Parameter	Value of model A	Value of model B
Viewing angle, ζ (deg)	169.07 ± 0.22	$168.50^{+0.26}_{-0.21}$
Initial wobble angle, θ_0 (deg)	19.52 ± 0.38	$30.52^{+0.66}_{-0.74}$
Angle between the magnetic and symmetry axis, χ (deg)	173.34 ± 0.13	$171.37^{+0.20}_{-0.16}$
Initial phase of the precession, Φ_0 (deg)	45^{+5}_{-4}	108 ± 3
Constant ellipticity of the NS, ϵ_0	$(1.24\pm0.03)\times10^{-7}$	$(9.17\pm0.14)\times10^{-8}$
Initial ellipticity of the NS, ϵ_1	$(2.37\pm0.05)\times10^{-6}$	$(1.58\pm0.03)\times10^{-6}$
Ellipticity relaxation timescale, $\tau\epsilon$ (days)	19.55 ± 0.35	36.43 ± 0.46
Wobble angle decay timescale, τ_θ (days)	74.30 ± 0.26	—
Frictional coupling timescale, τ_c (s)	—	2.49 ± 0.01
Ratio between the moment of inertia of the crust and the core, κ	—	<0.01
Start time of the precession, T_0 (MJD)	$58{,}444.5\pm0.4$	$58{,}444.9\pm0.5$
Initial twist parameter, n_0	$0.040^{+0.008}_{-0.040}$	$0.062^{+0.015}_{-0.062}$
Twisted magnetic field relaxation timescale, τ_t (days)	>1,500	>1,500

Modulations on polarized X-ray

- **Surface emission from magnetar is thought as highly polarized**

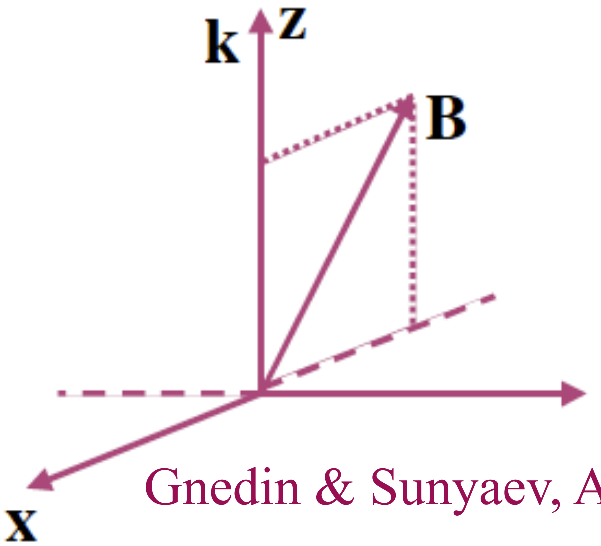

Gnedin & Sunyaev, A&A, 1974

Pavlov & Zavlin, ApJ, 2000

O-mode **E** nearly in the **k – B** plane

X-mode **E** nearly $\perp$ **k – B** plane

$$\kappa_{\mathrm{O}} \sim \kappa_{(B=0)} \quad \kappa_{\mathrm{X}} \sim \kappa_{(B=0)} \left(\omega/\omega_{ce}\right)^2$$

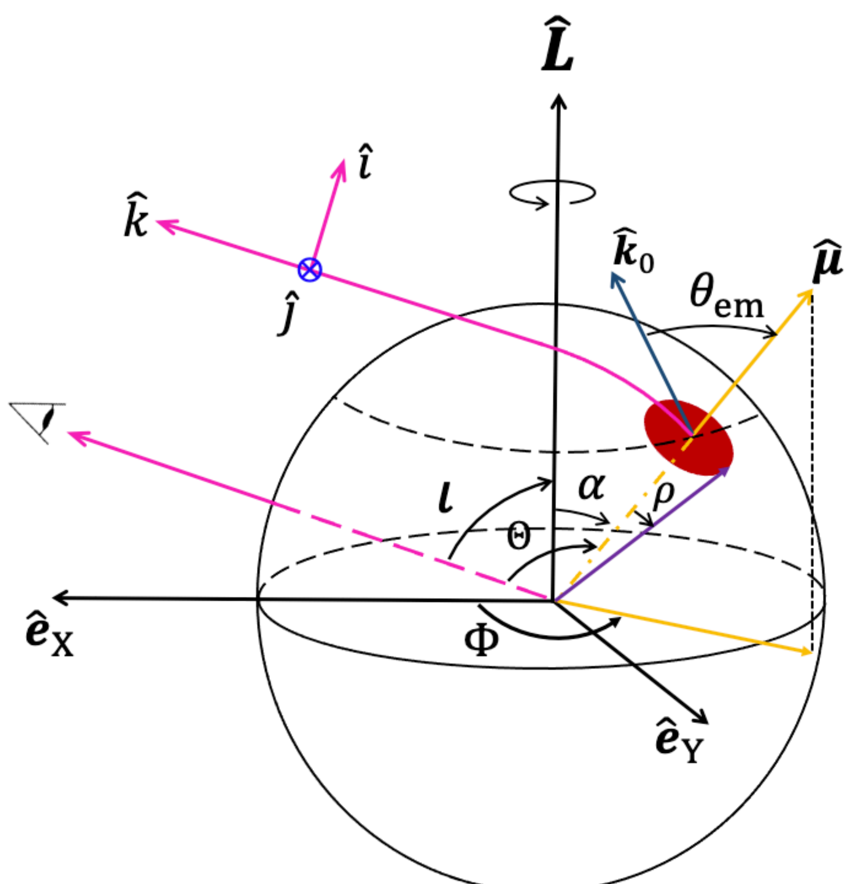

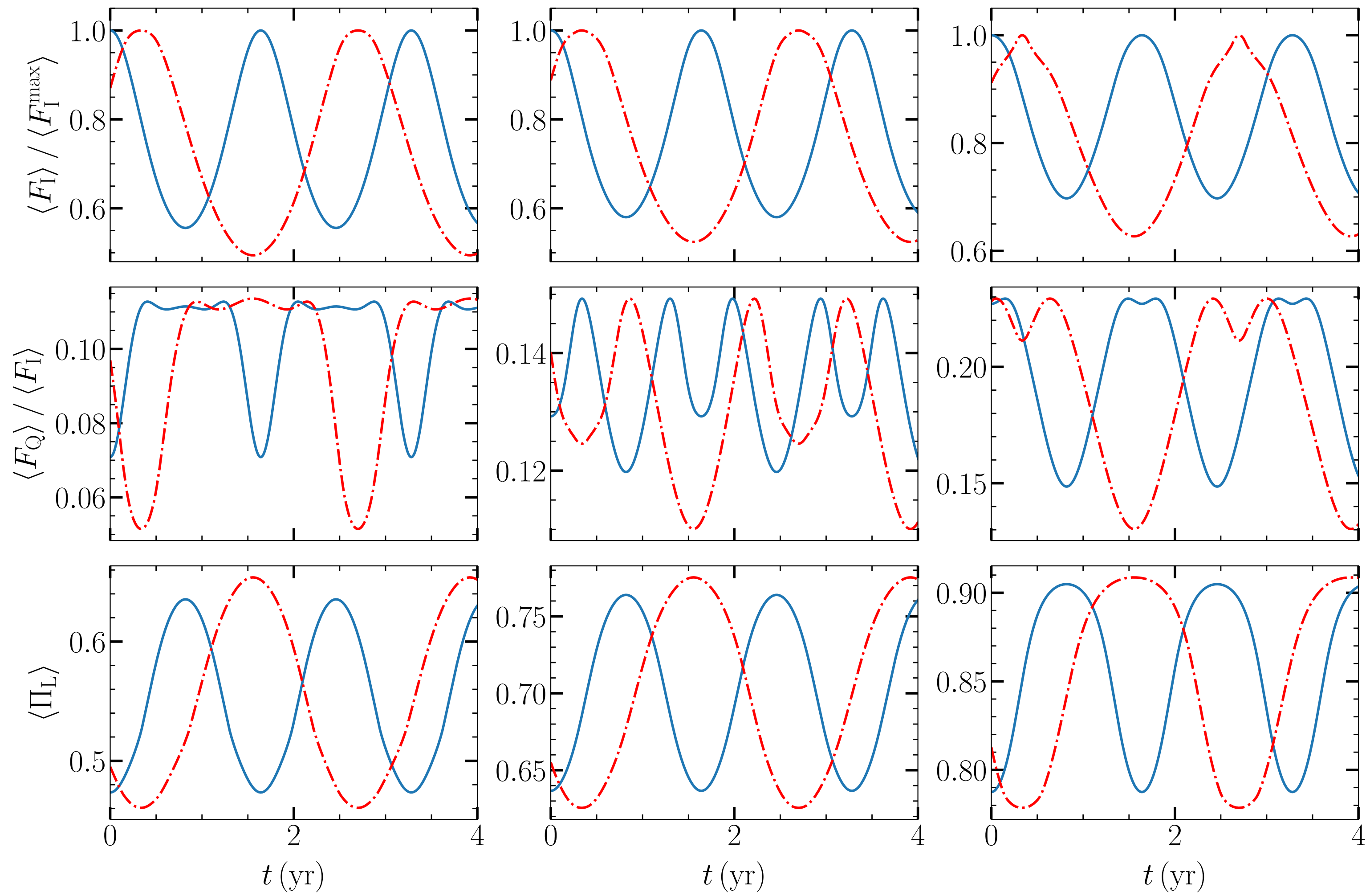

Gao et al., MNRAS, 2023

The effects of vacuum birefringence

What if the X-ray radiation comes from different patches on the NS surface or even the whole star?

The modulations on the flux may be "destroyed," but polarization is different

QED effect ($B > B_c = 4.4 \times 10^{13}$ G)

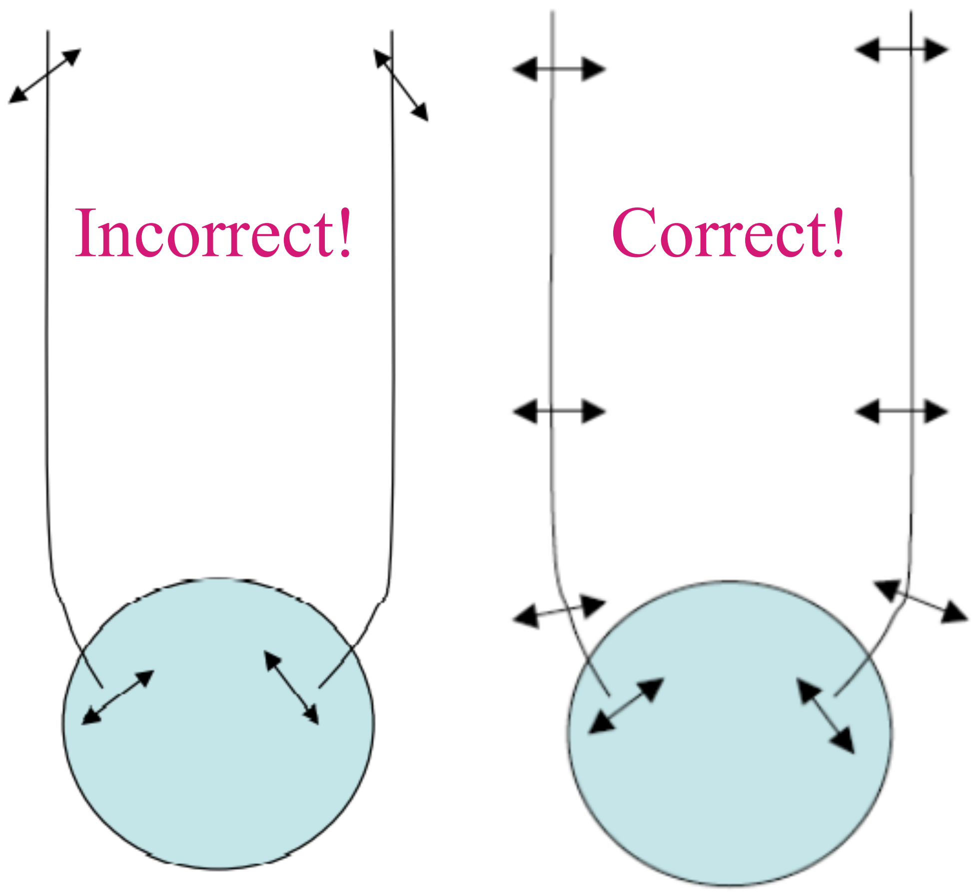

Credit: Dong Lai

- Evolve adiabatically along the direction of the magnetic field up to the "polarization limiting radius"

Heyl & Shaviv, PRD, 2002; Lai & Ho, PRL, 2003

- The polarization state can still vary periodically in the precession condition
- IXPE has conducted first observation of magnetar 4U 0142+61 X-ray polarization

Taverna et al., Science, 2022

Dynamical tides of inspiralling binary NSs

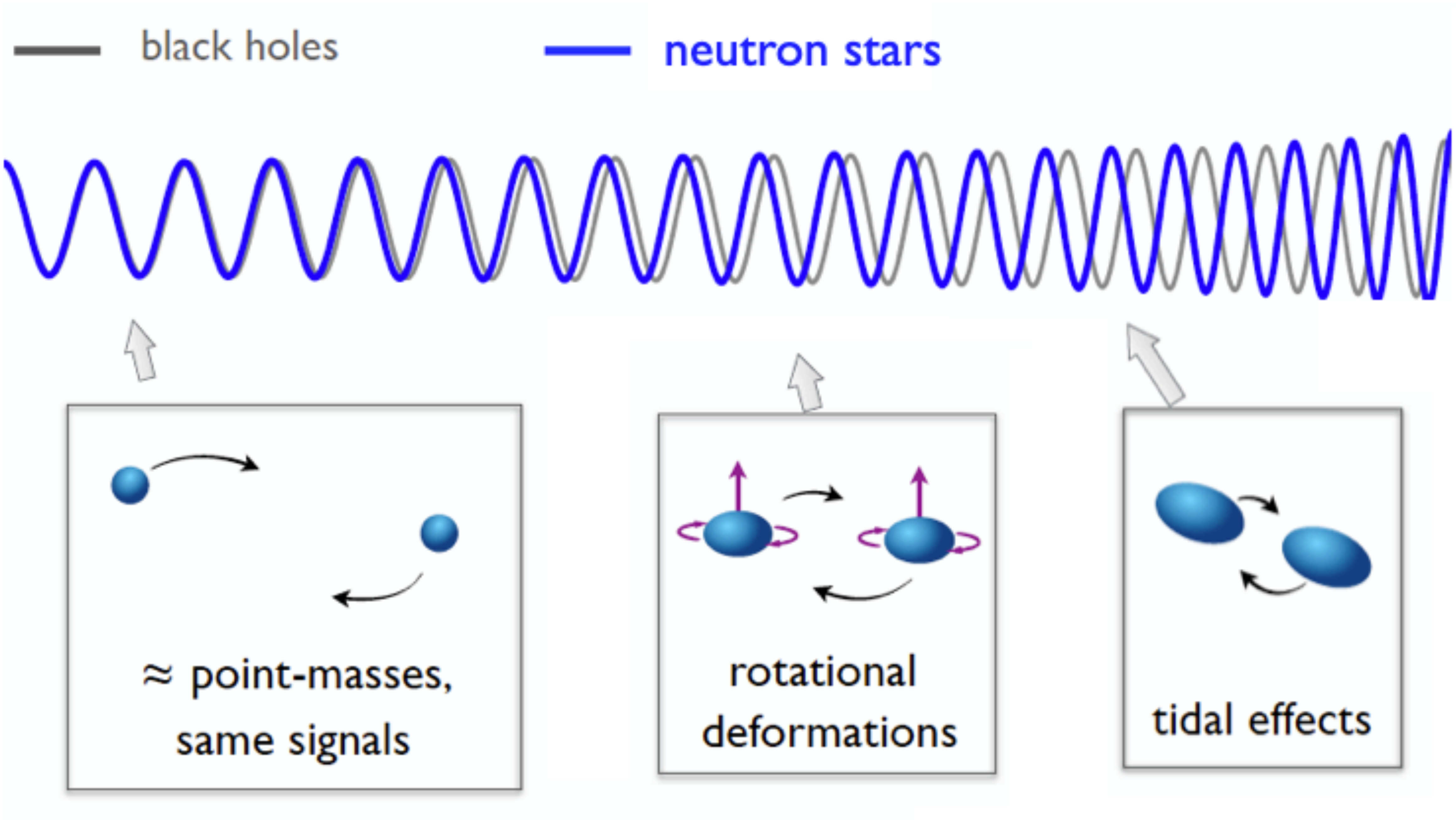

+ Tidal excitation of various oscillation mode

Dynamical tides of inspiralling binary NSs

$$\left(\rho\frac{\partial^2}{\partial t^2}+\mathscr{L}\right)\vec{\xi}=-\rho\nabla U \qquad U=-GM'\sum_{lm}W_{lm}\frac{r^l}{D(t)^{l+1}}e^{-im\Phi(t)}Y_{lm}(\theta,\phi)$$

Dong Lai, MNRAS, 1994

$$\vec{\xi}(\mathbf{r},t)=\sum a_\alpha(t)\vec{\xi}_\alpha(\mathbf{r}) \qquad \left(\mathscr{L}-\rho\omega_\alpha^2\right)\vec{\xi}_\alpha(\mathbf{r})=0$$

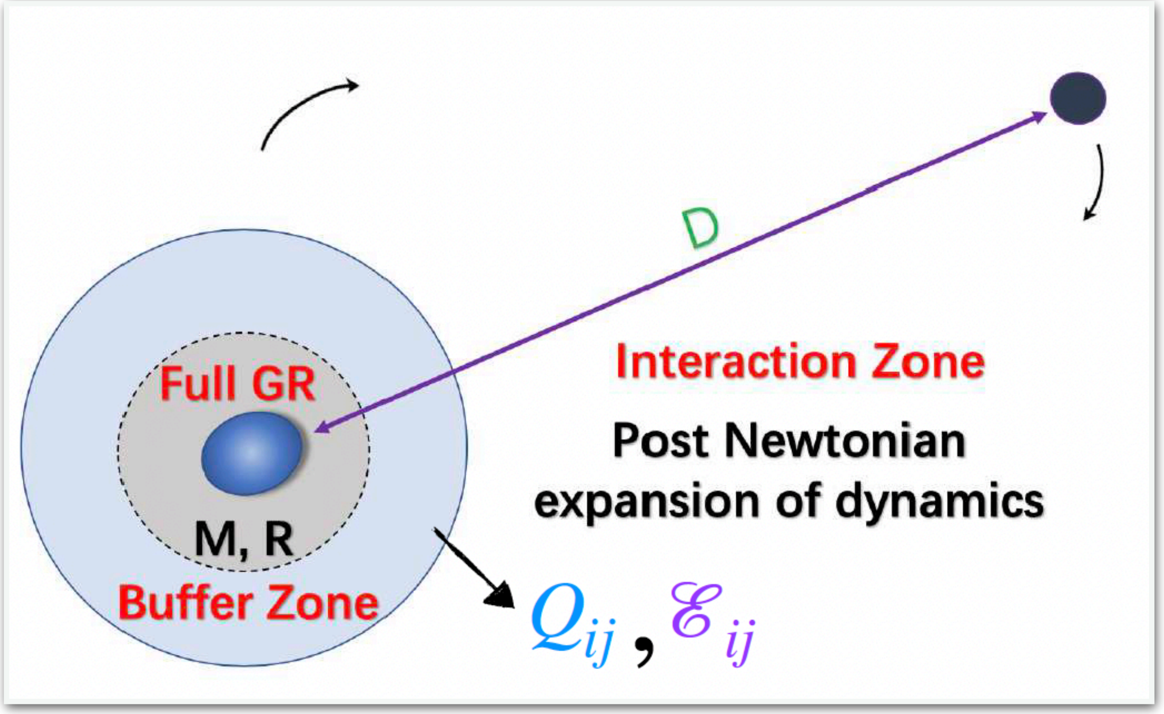

$$\ddot{a}_\alpha+\omega_\alpha^2 a_\alpha=\frac{GM_2W_{lm}Q_\alpha}{D^{l+1}}e^{-im\Omega_{\rm ort}t}$$

$$Q_{nl}=\int d^3x\rho\xi^*_{nlm}\cdot\nabla\left[r^lY_{lm}(\theta,\phi)\right]$$

$$=\int_0^R \rho l r^{l+1}\,dr\left[\xi^r_{nl}(r)+(l+1)\xi^1_{nl}(r)\right]$$

Tidal overlapping function

Static/adiabatic tides

$$\omega_\alpha \gg m\Omega_{\rm orb} \qquad a_\alpha\sim\frac{e^{i\Omega_{\rm orb}t}}{\omega_\alpha^2D^{l+1}}$$

Dynamical tides (resonance)

$$a_\alpha\sim\frac{e^{i\Omega_{\rm orb}t}}{\left(\omega_\alpha^2-m^2\Omega_{\rm orb}^2\right)D^{l+1}}$$

Dynamical tides of inspiralling binary NSs

GWs from oscillations are faint, only detectable (possibly) for supernova or pulsar glitch process

$$t_{\rm res} \simeq 0.01s\mathscr{M}_{1.2}^{-5/6}f_{600}^{-11/6} \ll t_D \simeq 0.1s\mathscr{M}_{1.2}^{-5/3}f_{600}^{-8/3}$$

The energy transferred from orbital to oscillation

$$\Delta E \simeq 5\times 10^{49}\,\mathrm{erg}\, f_{600}^{1/3}Q_{0.01}^{2}M_{1.4}^{-2/3}R_{12}^{2}q\left(\frac{2}{1+q}\right)^{5/3}$$

Phase shift in gravitational waves

$$\delta\Phi = \frac{\omega_{\rm mode}\Delta E}{P_{GW}} \simeq -0.12 f_{600}^{-2}Q_{0.01}^{2}M_{1.4}^{-4}R_{12}^{2}\frac{2q}{1+q}$$

Dynamical tides of inspiralling binary NSs

$$a_\alpha \sim \frac{e^{i\Omega_{\rm orb}t}}{\left(\omega_\alpha^2 - m^2\Omega_{\rm orb}^2\right) D^{l+1}}$$

$$\begin{aligned} Q_{nl} &= \int \mathrm{d}^3x \rho \xi^*_{nlm} \cdot \nabla\left[r^l Y_{lm}(\theta,\phi)\right] \\ &= \int_0^R \rho l r^{l+1}\, \mathrm{d}r \left[\xi^r_{nl}(r) + (l+1)\xi^1_{nl}(r)\right] \end{aligned}$$

Two things matter: mode oscillation frequency and tidal overlapping function, ideal case: low frequency and large overlapping function (eigenfunction should be as similar as r^l)

For spherical two component NSs (solid crust and fluid core), we mainly have the following fluid/solid oscillation mode

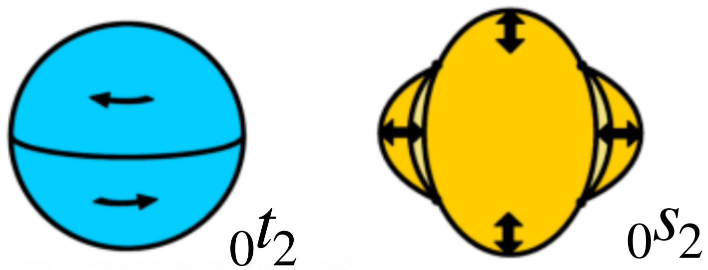

- **Shear (*s*,*t*) modes:** driven by elastic forces in the crust.
- **Pressure (*p*) modes:** driven by pressure.
- **Fundamental (*f*) mode:** (aka “Kelvin mode”) the first (nodeless) *p*-mode.
- **Gravity (*g*) modes:** driven by buoyancy (thermal/composition gradients).

Dynamical tides of inspiralling binary NSs

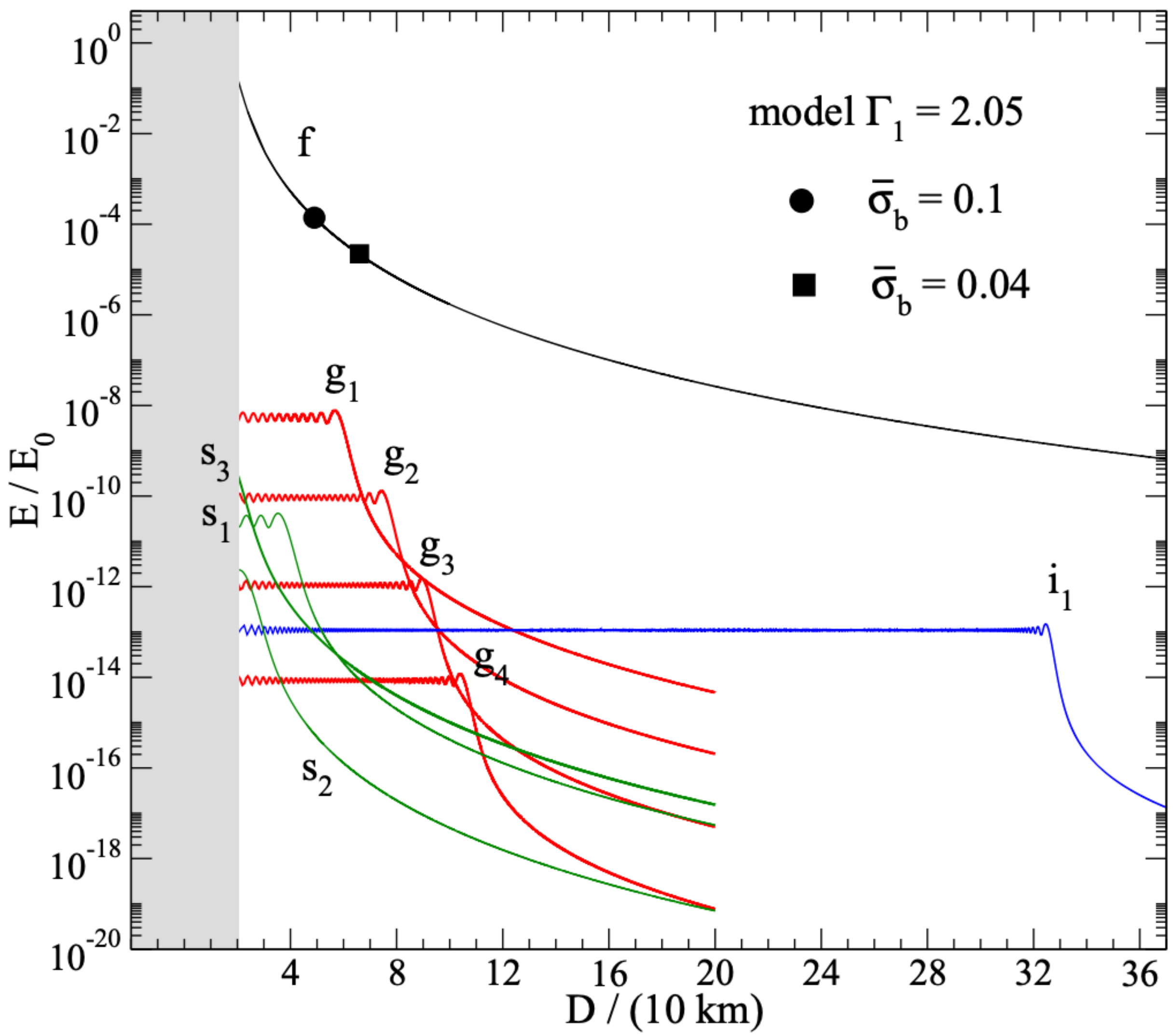

Pasamonti & Andersson, MNRAS, 2021

Mode	$\tilde{\omega}_n$	$\lvert\tilde{Q}_n\rvert$
p_4	9.1741	4.3149×10^{-5}
p_3	7.3626	2.9863×10^{-4}
p_2	5.4963	2.5463×10^{-3}
p_1	3.5206	2.5858×10^{-2}
f	1.2274	5.5795×10^{-1}
g_1	0.1848	1.7435×10^{-3}
g_2	0.1277	3.7451×10^{-4}
g_3	0.0983	6.1782×10^{-5}
g_4	0.0796	1.0704×10^{-5}
g_5	0.0664	2.3809×10^{-5}
s_1	0.3403	5.9732×10^{-4}
s_2	0.6212	2.2991×10^{-4}
s_3	0.9016	1.1045×10^{-3}
s_4	1.1817	3.0456×10^{-3}
s_5	1.4615	1.1796×10^{-3}
s_6	1.7412	2.5158×10^{-4}
i_1	0.0151	4.0293×10^{-6}

$$E = E_k + E_p = \frac{1}{2} \sum \mathscr{A}_n^2 \left(\left| \dot{a}_n(t) \right|^2 + \omega_n^2 \left| a_n(t) \right|^2 \right)$$

Dynamical tides of inspiralling binary NSs

Interfacial mode: due to discontinuity in density (g mode) or shear modulus

$$f_N = g_N \rho \frac{dp}{dr}\left(\frac{1}{\Gamma_0 p} - \frac{1}{\rho}\frac{\Delta\rho}{\Delta p}\right)\delta r \qquad \gamma \equiv \frac{\Delta p}{\Delta\rho}\frac{\rho + p}{p}$$

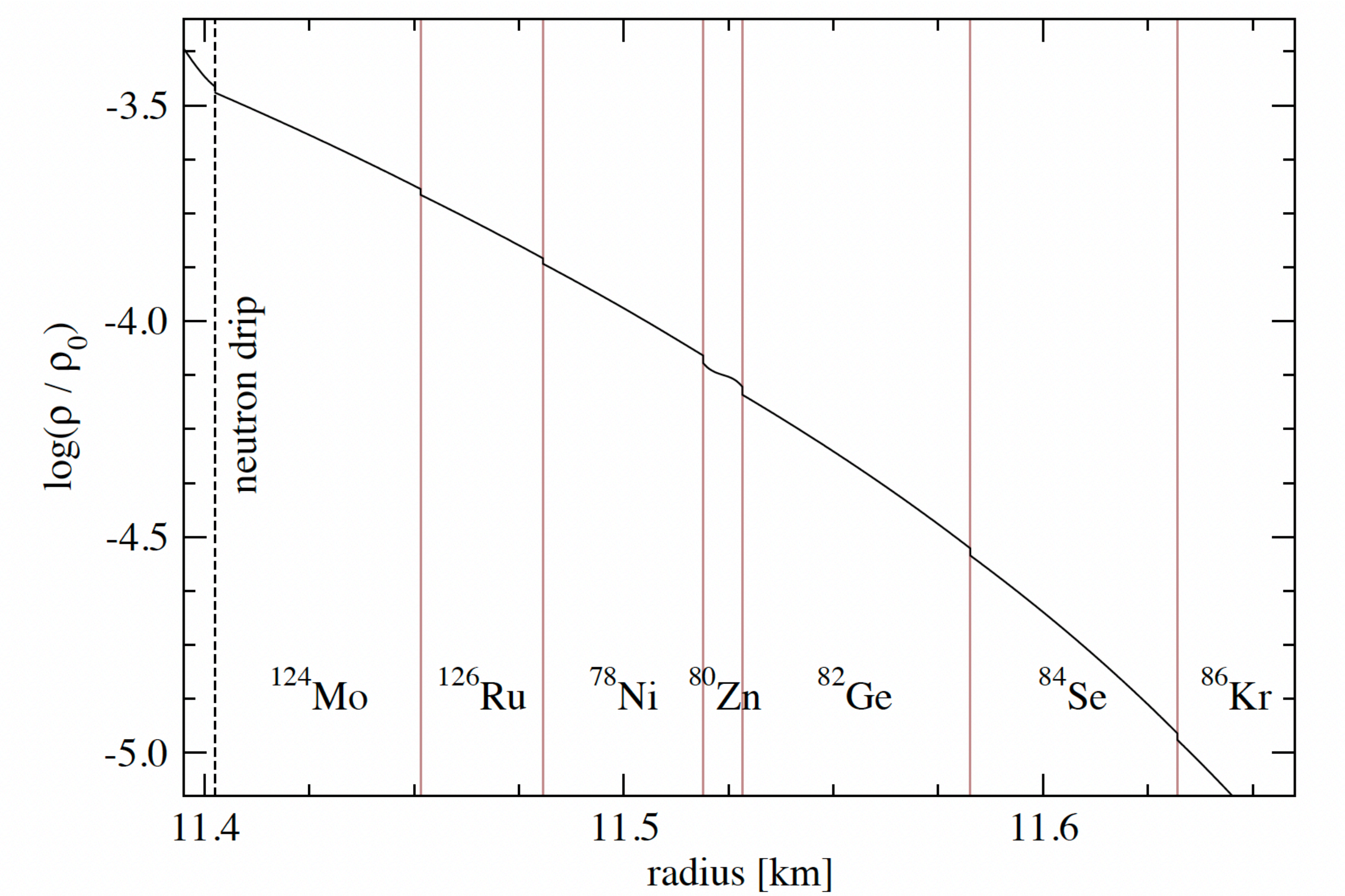

Finn, MNRAS, 1987

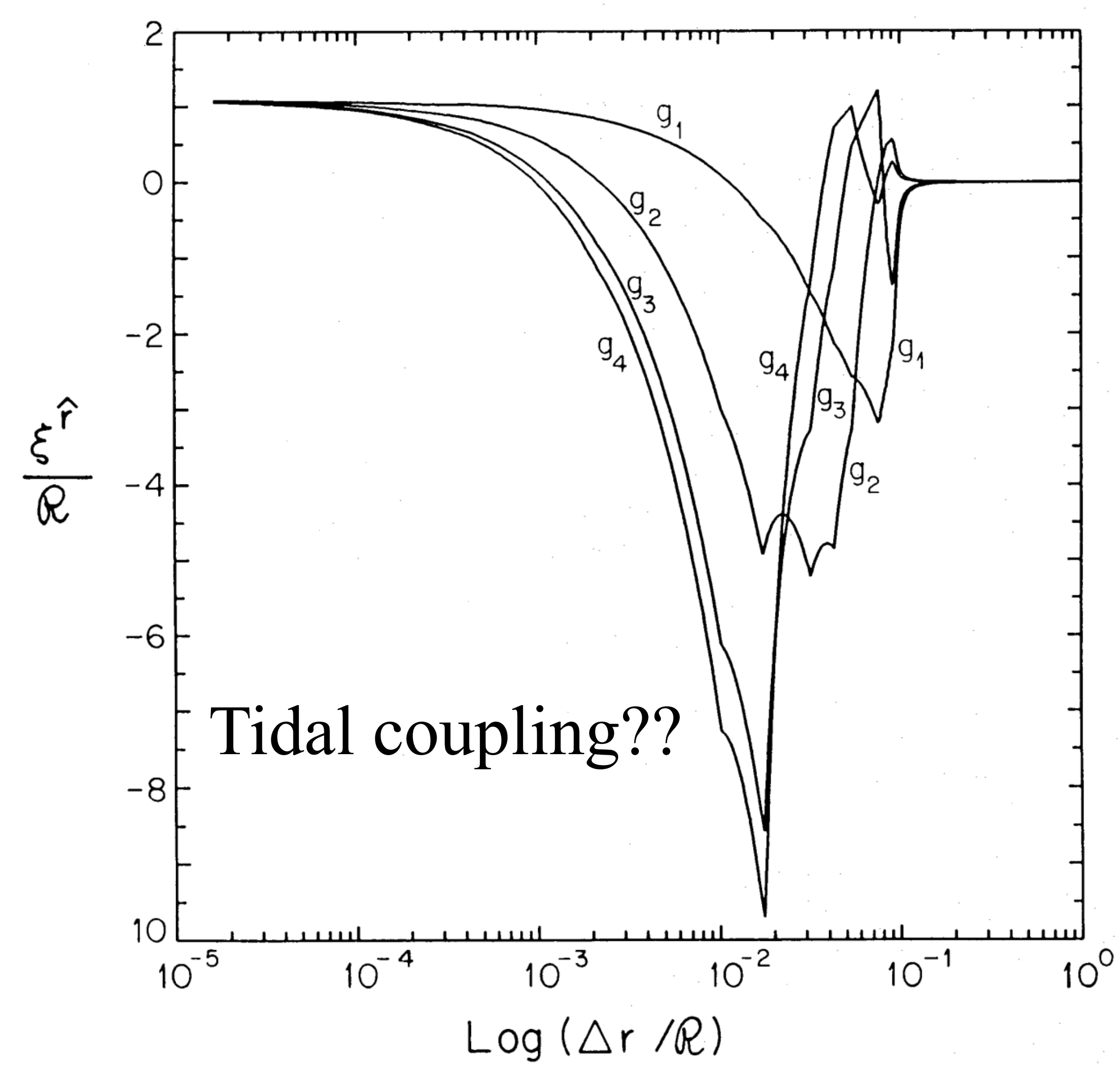

Dynamical tides of inspiralling binary NSs

Interfacial mode: due to discontinuity in density (g mode) or shear modulus

Tonetto & Lugnes, PRD, 2020   Miao et al., ApJ, 2024

$$f_{\mathrm{N}} = g_{\mathrm{N}}\rho\frac{dp}{dr}\left(\frac{1}{\Gamma_0 p} - \frac{1}{\rho}\frac{\Delta\rho}{\Delta p}\right)\delta r$$

$$\omega^2 \propto \frac{\Delta\varepsilon}{\varepsilon_t}\frac{\Delta R}{R}\frac{GM}{R^3}$$

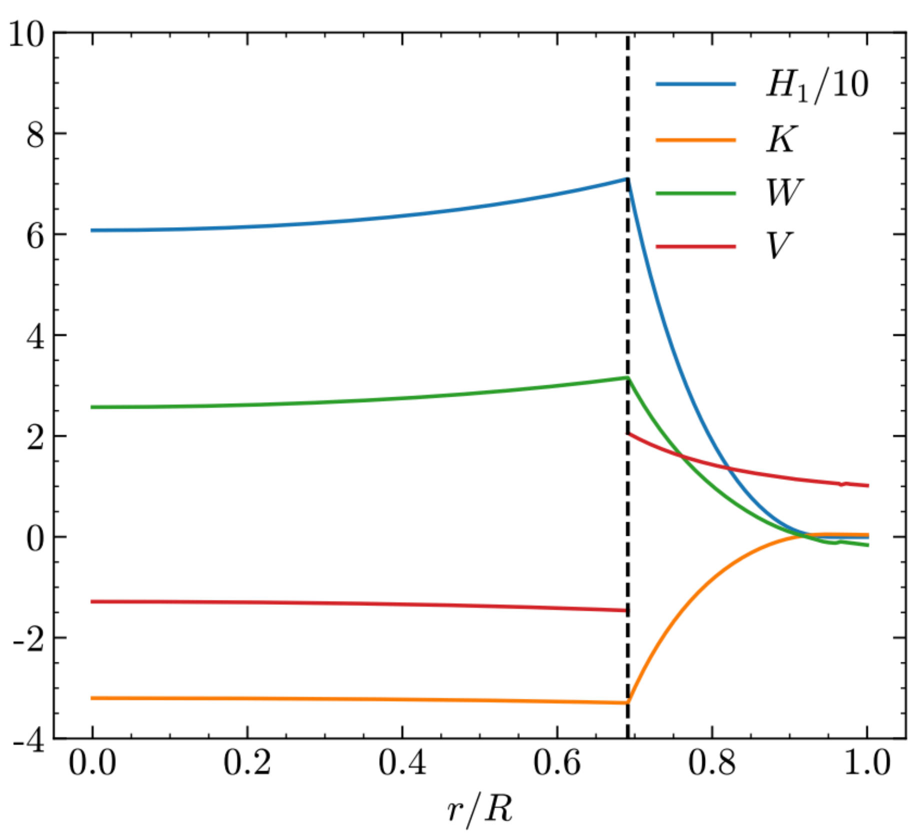

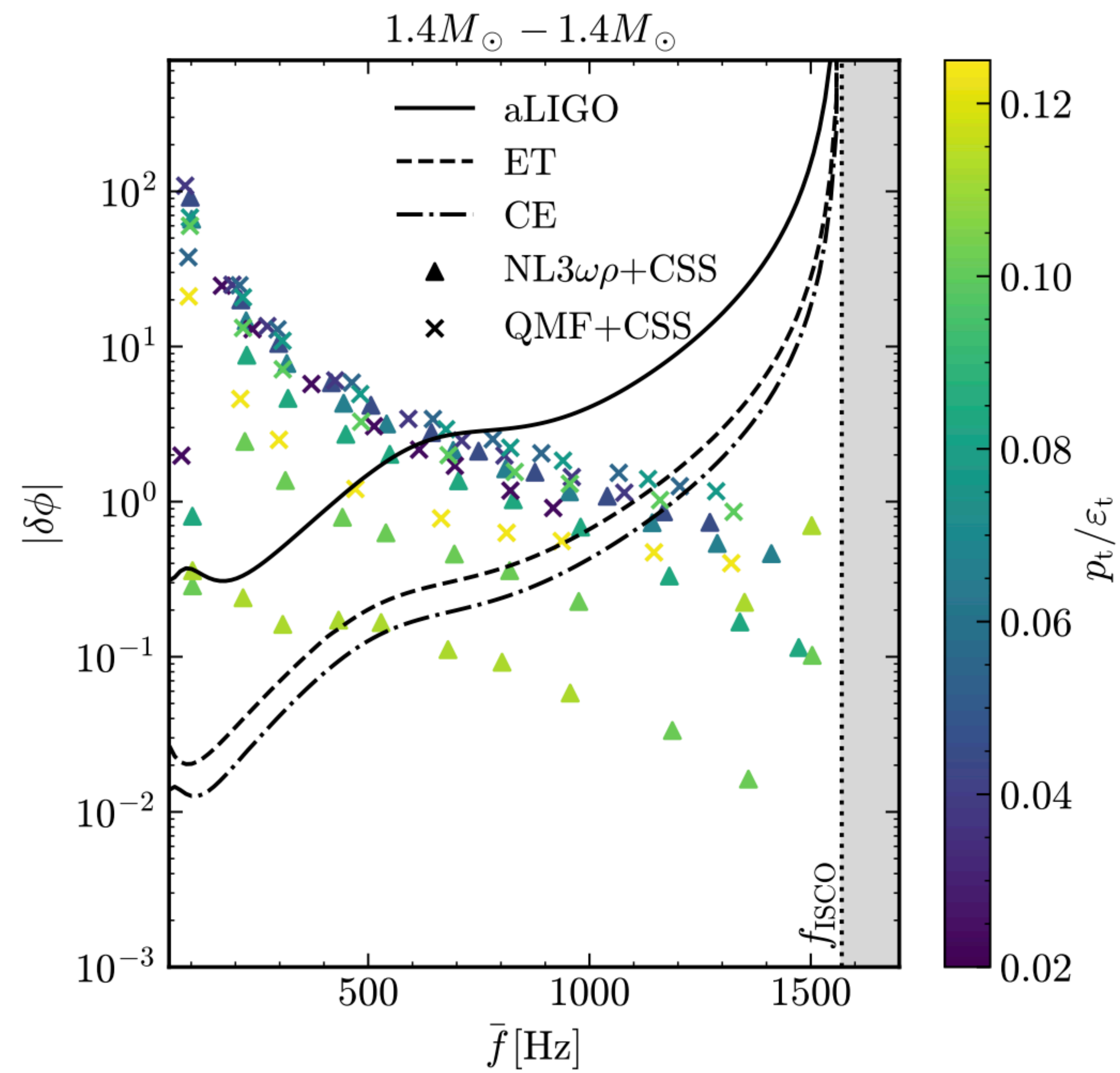

Dynamical tides of inspiralling binary NSs

Interfacial mode: due to discontinuity in density (g mode) or shear modulus

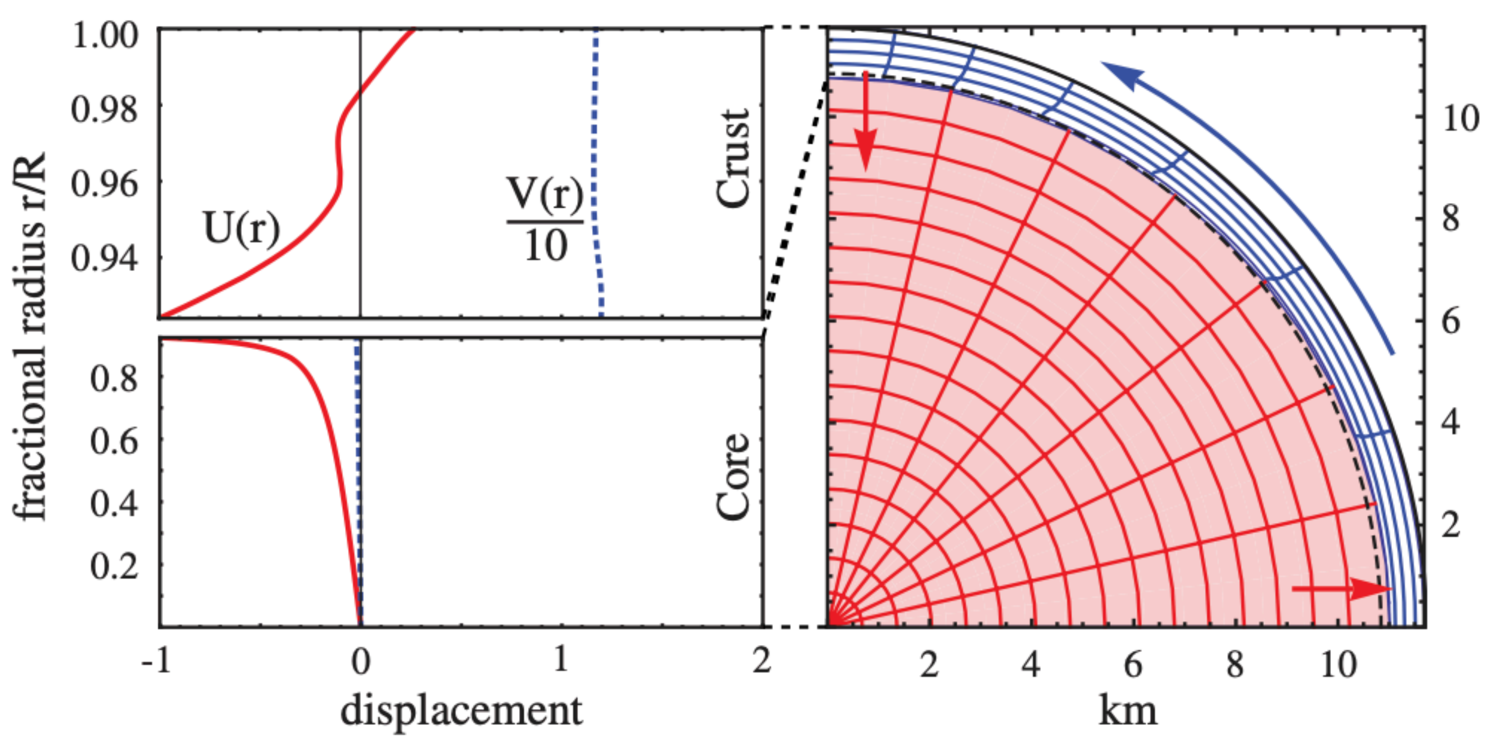

EOS	$f_{\rm mode}$ [Hz]	Q
SLy4	188	0.041
APR	170	0.061
SkI6	67.3	0.017
SkO	69.1	0.053
Rs	32.0	0.059
Gs	28.8	0.060

Tsang et al., PRL, 2012; Pan et al., PRL, 2020

$$E_{\rm max} \simeq 5\times10^{50}\,{\rm erg}\, f_{188}^{1/3} Q_{0.04}^{2} M_{1.4}^{-2/3} R_{12}^{2} q \left(\frac{2}{1+q}\right)^{5/3}$$

Energy to crack the crust

$$E_b = \left(2\pi f_{\rm mode}\right)^2 \int d^3x \rho \xi_b^* \cdot \boldsymbol{\xi}_b \simeq 5\times10^{46}\,{\rm erg}\,\epsilon_{0.1}^2$$

Trigger global oscillation

$$\sim (\mu/\rho)^{1/2}/(2\pi\Delta r) \sim 200 \text{ Hz}$$

Dynamical tides of inspiralling binary NSs

Interfacial mode due to discontinuity in shear modulus

1. Relativistic calculations of the oscillation frequency is important (eg., 50Hz and 150Hz resonance are very different)

$$\Delta E \simeq 5 \times 10^{49}\,\mathrm{erg}\, f_{600}^{1/3} Q_{0.01}^{2} M_{1.4}^{-2/3} R_{12}^{2} q \left(\frac{2}{1+q}\right)^{5/3}$$

$$\delta\Phi = \frac{\omega_{\mathrm{mode}} \Delta E}{P_{GW}} \simeq -0.12 f_{600}^{-2} Q_{0.01}^{2} M_{1.4}^{-4} R_{12}^{2} \frac{2q}{1+q}$$

2. Hybrid method (GR background + Newtonian Cowling approximation of the oscillation) cannot guarantee the orthogonality of different modes, for example, eigenfunction of f-mode “enters into”inside other modes, causing large wrong tidal overlapping function

Lai, MNRAS, 1994; Passamonti & Andersson, MNRAS, 2021; Miao et al., ApJ, 2023

General relativistic perturbation theory

$$\xi^\mu = r^l \begin{pmatrix} 0 \\ W r^{-1} e^{-\lambda/2} \\ -V r^{-2} \partial_\theta \\ -\frac{V}{r^2 \sin^2\theta} \partial_\phi \end{pmatrix} P_l(\cos\theta) e^{i\omega t}$$

$$\delta g_{\mu\nu} = -r^l \begin{pmatrix} H_0 e^\nu & i\omega r H_1 & 0 & 0 \\ i\omega r H_1 & H_2 e^\lambda & 0 & 0 \\ 0 & 0 & r^2 K & 0 \\ 0 & 0 & 0 & r^2 \sin^2\theta K \end{pmatrix} P_l(\cos\theta) e^{i\omega t}$$

Strain tensor

$$\delta s_\mu^\nu = \frac{1}{2} \left(\perp_\mu^\sigma \perp^{\lambda\nu} - \frac{1}{3} \perp_\mu^\nu \perp^{\sigma\lambda} \right) \Delta g_{\sigma\lambda}$$

Stress tensor

$$\delta \pi_\mu^\nu = -2\check{\mu}\delta s_\mu^\nu$$

$$T_1 := \delta\pi_r^r \quad \textit{and} \quad T_2 := \delta\pi_r^\theta$$

$$\delta T_{\mu\nu}^{\text{tot}} = \delta T_{\mu\nu} + \delta\pi_{\mu\nu}$$

$$\delta G_{\mu\nu} = 8\pi\delta T_{\mu\nu} \quad \text{and} \quad \delta\left(\nabla_\mu T^{\mu\nu}\right) = 0$$

Detweiler & Lindblom, ApJ, 1983,1985; Charger & Andersson, PRD, 2015

General relativistic perturbation theory

$$H_1' = \left[\frac{1}{2}(\lambda' - \nu') - \frac{l+1}{r}\right] H_1 + \frac{e^\lambda}{r}\left[H_2 + K - 16\pi(\rho + p)V\right],$$

$$K' = \frac{1}{r}H_2 + \frac{n+1}{r}H_1 + \left[\frac{1}{2}\nu' - \frac{l+1}{r}\right]K - \frac{8\pi}{r}e^{\lambda/2}(\rho+p)W,$$

$$H_0' = K' - re^{-\nu}\omega^2 H_1 - \left[\frac{1}{2}\nu' + \frac{l-1}{r}\right]H_0 - \left[\frac{1}{2}\nu' + \frac{1}{r}\right]H_2 + \frac{l}{r}K - \frac{16\pi}{r}T_2,$$

$$W' = -\frac{l+1}{r}W + re^{\lambda/2}\left[\frac{e^{-\nu/2}}{\gamma p}X - \frac{l(l+1)}{r^2}V + \frac{1}{2}H_2 + K\right],$$

$$V' = \frac{1}{2\check{\mu} r}T_2 + \frac{e^{\lambda/2}}{r}W + \frac{2-l}{r}V,$$

$$T_2' = -\frac{1}{2}re^\lambda(\rho+p)H_0 + \left[\frac{4ne^\lambda\check{\mu}}{r} - e^{\lambda-\nu}r\omega^2(\rho+p)\right]V + e^{\lambda/2}p'W$$
$$+ re^{\lambda-\nu/2}\left(X - \frac{1}{2r^2}e^{\nu/2}T_1\right) + \left[\frac{1}{2}(\lambda'-\nu') - \frac{l+1}{r}\right]T_2.$$

$$H_2 = H_0 + 64\pi\check{\mu}V,$$

$$\left[\frac{re^{-\lambda}}{2}(r\nu' - 2) + (n+1)r\right]H_0 = r^2e^{-\lambda}\left[\omega^2 re^{-\nu} - \frac{n+1}{2}\nu'\right]H_1$$
$$+ \left[nr - \omega^2 r^3 e^{-\nu} - \frac{1}{4}r^2e^{-\lambda}\nu'(r\nu' - 2)\right]K$$
$$+ 8\pi r^3 e^{-\nu/2}X + 8\pi r T_1 - 16\pi r e^{-\lambda}T_2,$$

$$\frac{2}{3}e^{-\nu/2}\check{\mu}r^2 X - \frac{1}{4}\gamma p T_1 = \check{\mu}\gamma p\left[2e^{-\lambda/2}W - r^2K + l(l+1)V\right].$$

Joint condition

$$[H_0]_r = [H_1]_r = [K]_r = 0$$

	fluid	elastic
fluid	$[W]_r = 0$	$[W]_r = 0$ $[T_2]_r = 0$
elastic	$[W]_r = 0$ $[T_2]_r = 0$	$[W]_r = 0$ $[V]_r = 0$ $[T_2]_r = 0$

How to solve the system?

1. Center and surface boundary conditions for a given ω

2. The quasi normal mode only have outgoing gravitational waves

Summary

1. Global properties can give us constraints on EoS, but hard to give decisive answer

2. Modeled the dynamical evolution, timing, polarized emission of precessing NSs (searching template)

3. Found evidence of damped precession, deformation is consistent with current understanding of crust elasticity or high magnetic field, but the damping mechanism is still not clear (internal coupling or decreasing ellipticity)

Ongoing: modeling including complex deformation and damping

4. Dynamical tides can be used to probe the solid phase of NSs, but the detailed modeling within GR perturbation is still lacking.

Still need to do: Compare with Newtonian ones, EoS dependence, energy budget for crust shattering, GW phase contribution

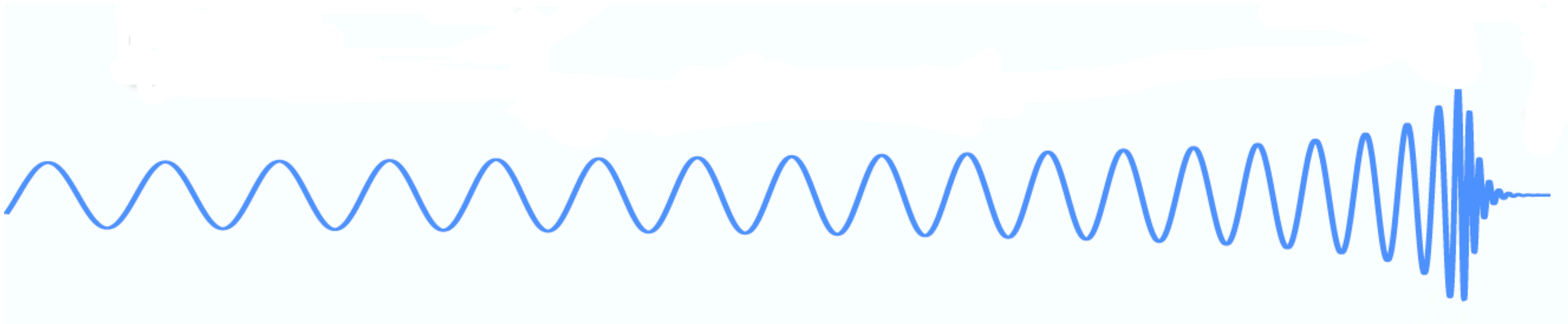

Thank you for listening!